UNL ROCKETRY TEAM

Flight Readiness Review

2011-2012
NASA University Student Launch Initiative

University of Nebraska-Lincoln

Table of Contents

1.0 Summary of FRR Report

1.1 Team Summary

University of Nebraska – Lincoln Rocketry Team		
Location:	Lincoln, Nebraska	
Faculty Advisor:	Dr. Kevin Cole	Professor-Mechanical and Materials Engineering
Certified Mentor :	Thomas Kernes	National Association of Rocketry #82141
Project Director:	Matthew Mahlin	
Payload Team Leader:	Alexandra Toftul	
Safety Coordinator:	Paul Kubitschek	

1.2 Launch Vehicle Summary

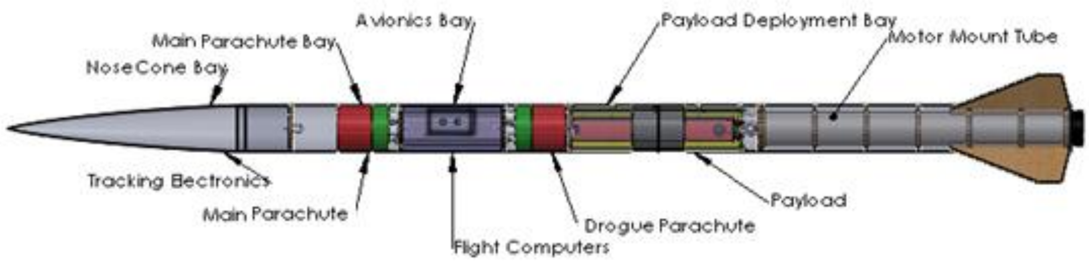

Length:	124.5”	
Diameter:	5.5”	
Nose Cone:	27.5”	Von Kármán (LD-Haack), 1:5 Fineness
Fin Span:	14.5”	(3-fin configuration)
Weight:	23.7 lbs	(No Motor – No Payload)
Motor Mount:	98mm	37” long – rear retaining ring

Selected Motor:

Designation	Total Impulse (N*S)	Thrust/Weight	Maximum Payload (lbm)	Rail (in)
L1170FJ-P	4214	6.82/1	5	144

Recovery System:

Component	Characteristic Dimension	Comment
Main Parachute	108”	Hemispherical with 24” Spill hole
Drogue	36”	Mach 1 Ballistic X-Form
Shock Cord	52’ Main / 50’ Drogue	1” Tubular Nylon
Wadding	24”	2 x Fire resistant protective cloth

1.3 Payload Summary

The deployable payload will be designed to separate fully from the rocket and descend under a spiraling parafoil. The structure will house an experimental energy scavenging system, which will autonomously activate shortly after separation and will collect and transmit data throughout descent.

2.0 Changes Since Critical Design Review

2.1 Vehicle Criteria

The shock cord for the drogue has been increased from 30 to 50 feet to reduce forces on the payload.

2.2 Payload Criteria

Since the critical design review, the payload release has been changed from a servo actuated release to a dual deployment link. This device is essentially an explosive bolt that keeps the parafoil packaged and the payload connected to the shock cord. The dual deployment link was selected because it was designed to handle high load deployment.

In addition to the deployed payload, a wireless telemetry and video system was added to the vehicle's nosecone. This will provide live data, including GPS information, and video to the ground station during flight. This system transmits at 2.4 GHz to a servo controlled tracking station that feeds the live video to a laptop to be recorded. Originally, a video system was considered for the deployable payload but was removed due to size constraints. Thus, the system has been reintegrated as the communication system of the rocket itself.

2.3 Activity Plan

Team activities for testing have been completed with some minor alterations to the schedule. Of primary concern was the team's full scale test launch which had to be moved from March 17th to March 24th because of winds gusting to 36 mph at the launch site. Additionally, the rocket motor that we used for our test launch was also changed because Aerotech was simply unable to ship. So, we were forced to use an alternative motor made available by the local rocketry club.

Unfortunately, several original team members were unable to participate in the project due to other commitments. This has resulted in much of the work to be taken over by just four members. Although we've had to work harder than anticipated, the team is still on track.

The team's outreach activities continued to engage middle school students at Park Middle School in water rocketry. The number of students engaged has reached 121 in total. For the first educational engagement, students were taught the basics of rocketry, built their own water rockets, and launched them after three sessions. The second educational engagement focused on using the subscale and full-scale rockets and videos of their launches to teach the basics of rocketry. This concluded in students building stomp rockets.

3.0 Vehicle Criteria

3.1 Design and Construction of Launch Vehicle

3.1.1 Design and Construction

At this point in the project, the vehicle has gone through a test flight and has been successfully recovered. Construction of the vehicle was completed in January. Ejection charge testing concluded in February. The sub-scale and full-scale test flights were performed in March. The overall design of the vehicle was modeled in OpenRocket and Solidworks.

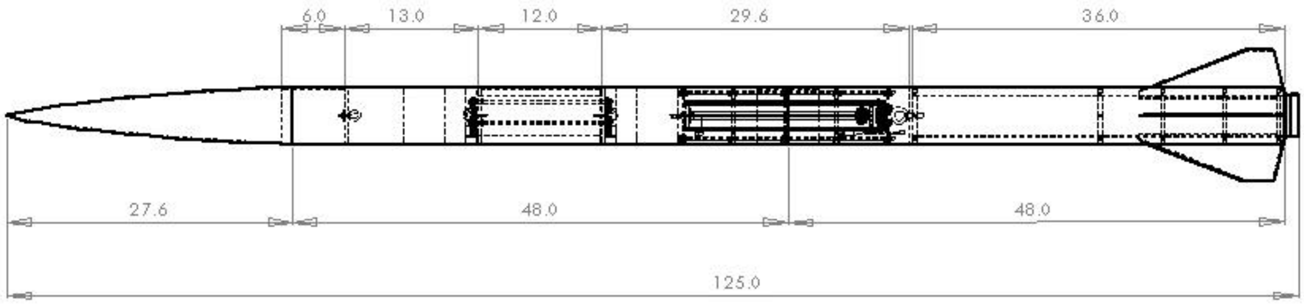

Figure 1 Dimensional Drawing of Entire Assembly.

A dimensional drawing of the entire assembly is provided in Fig. 1. Further dimensional drawings of the systems therein are provided for each section. An exploded assembly of the vehicle is shown in Fig. 2.

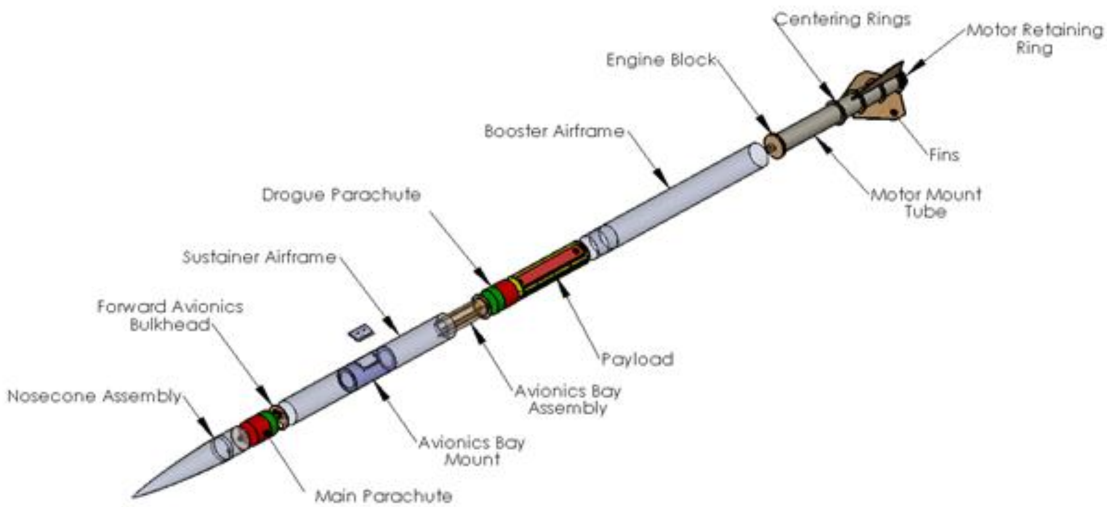

Figure 2 Exploded assembly of vehicle.

Nosecone

The Nosecone will be a minimum drag for the given diameter Von Kármán profile with a 5:1 fineness ratio. The dimensions are 27.5 inches in length cone with a 5.5 inch diameter base and the inside will be left hollow to allow room for tracking equipment. The materials will be a filament wound RF transparent fiberglass structure with a screw on aluminum tip. Finally, a 5 inch long shoulder at the base of this and capped with a screw in bulkhead to allow fitting and tethering to the top of the sustainer section.

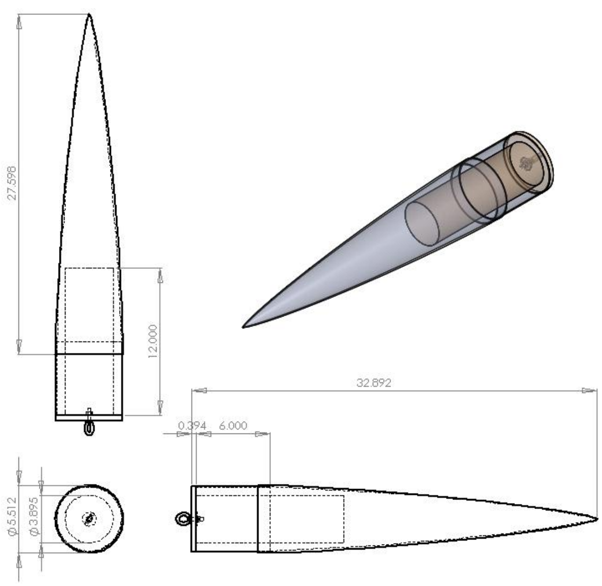

Figure 3 Nosecone drawing and model, dimensions are in inches.

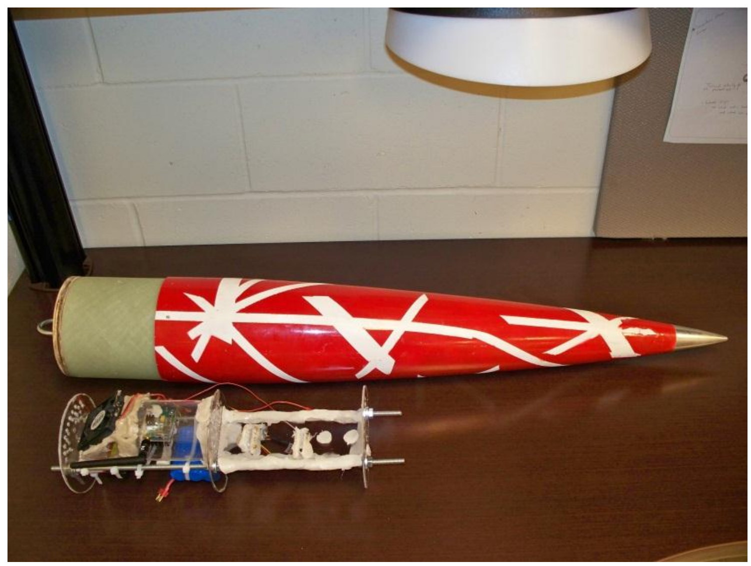

Figure 4 Finished Nosecone with communication electronics sled.

A length of ¼" all-thread rod extends from the screw on aluminum tip to the base of the bulkhead. This creates a direct connection from the nose tip to the bulkhead. A ¼" diameter U-Bolt with a back plate is bolted to this bulkhead. This forms the connection point for the main parachute. In order to connect the main, an 880lbf rated ¼" quick link is used to connect the shroud lines, U-bolt, and Shock cord.

Sustainer Assembly

The 4-foot long 5.5-inch diameter Body section has been constructed of Blue Tube reinforced with a fiberglass cloth for added fracture resistance and covered in a fine glass sock to create a smooth finish. The internal space is divided into three bays. The forward bay houses the Main Parachute with 52’ of tubular nylon shock cord and a nomex parachute protector. It is 13 inches long with the nosecone attached. Below the forward bay is the 12-inch long avionics bay that is compression mounted on to a fixed coupler tube segment. This coupler tube has been epoxied in to the middle of the frame to provide sufficient support area. Finally, the aft bay is the compartment housing the drogue parachute and the deployable payload. For maximum volume, the compartment will be open to the top of the Booster section creating a 29-inch long 5.2-inch diameter bay. An allowable 18 inches of this length have been allocated to payload volume with the remainder accommodating recovery components and recovery hard points.

In order to provide access to the avionics bay, the sustainer section has been outfitted with a hatch. The hatch is centered on the sustainer and measures 5 inches high and 3 inches wide. This allows the data ports of the flight computers to be accessed and the batteries to be charged without disassembling the avionics bay. The exterior of the hatch hold the two key switches for the dual flight computers. This hatch is fixed to the coupler mounted in the sustainer by four machine screws at the corners.

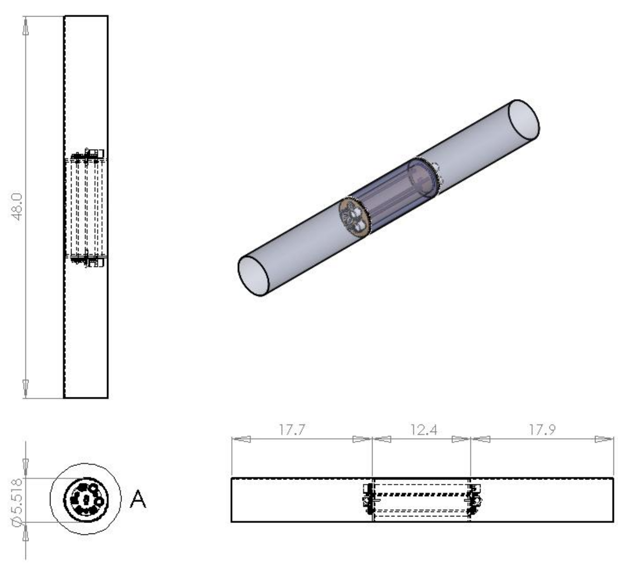

Figure 5 Sustainer Assembly with Avionics Bay. All dimensions are in inches.

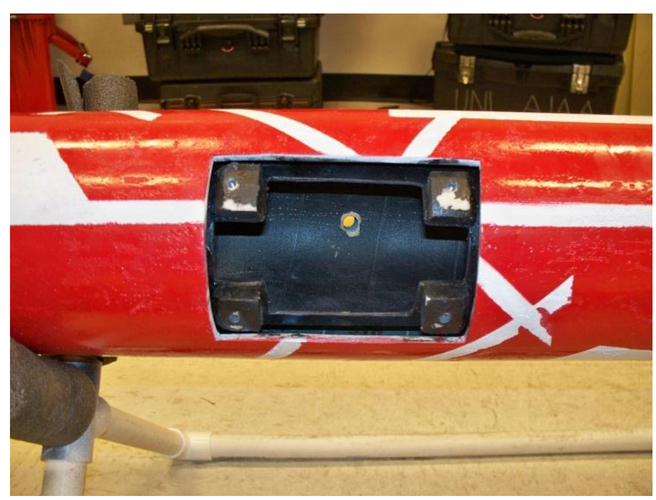

Figure 6 Avionics Bay access hatch with 4 locating screws.

Booster Assembly

The rearmost section will be referred to as the Booster and has been constructed in the same manner as the Body section before it. The two will be joined by a 6 inch coupler bonded to the Booster section. The purpose of this section is to contain and retain the motor. A 36-inch long, 98-mm motor mount tube was assembled with centering rings, engine block, and the three delta fins. The engine block at the top of the motor mount tube is composed of a half inch bulkhead reinforced with four layers of 8 oz. fiberglass at either side. The top of this is cemented and reinforced even more with a quarter inch thick layer of resin on top that is bonded to the engine block, parachute eyebolt, and interior of the airframe.

Fin slots are cut in the airframe tube and this motor mount assembly is bonded with epoxy to the lower 36 inches of the section. To further reinforce the connection, fiberglass fillets were built up at the joints between the airframe and fins. Then these were overlaid with two-4 oz. fiberglass sheets from fin tip to adjacent fin tip. Motors will be retained by the rear mounted cylindrical 98-mm machined aluminum Aero Pack motor retainer. This also allows a 98 to 75-mm adapter in our possession to be used to hold smaller diameter motors that will be used.

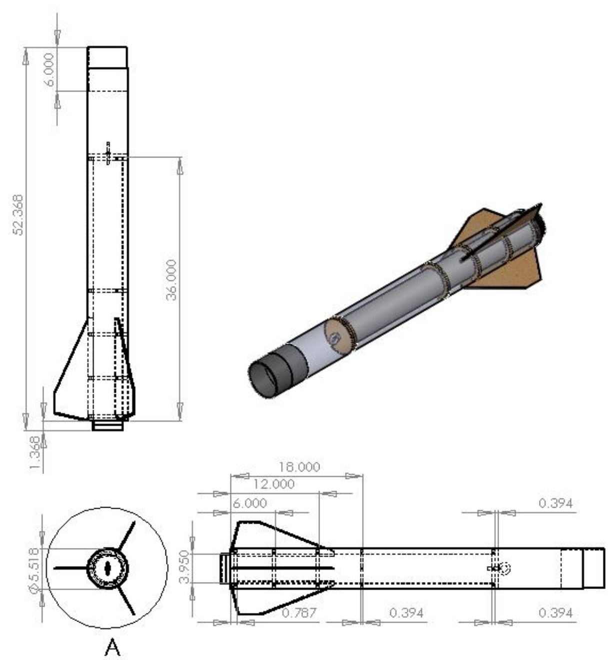

Figure 7 Booster Assembly with Fins and Motor Mount Tube. All dimensions are in inches.

Figure 8 Fins, centering rings, and motor mount tube after being epoxied together.

The fin profiles of the rocket were designed in OpenRocket. The delta is clipped to reduce the likelihood of breaking the tips. Each fin is made of three layer plywood. As this plywood is not reliably strong alone, each fin has been wrapped in two layers of 4-ounce fiberglass E-glass cloth and cured in a vacuum bag. The fins are mounted without a cant angle as a spin has been deemed undesirable for the payload. Fin alignment was facilitated by matching groves cut in the fins to corresponding ones cut in the centering rings mounted on the Motor Mount Tube.

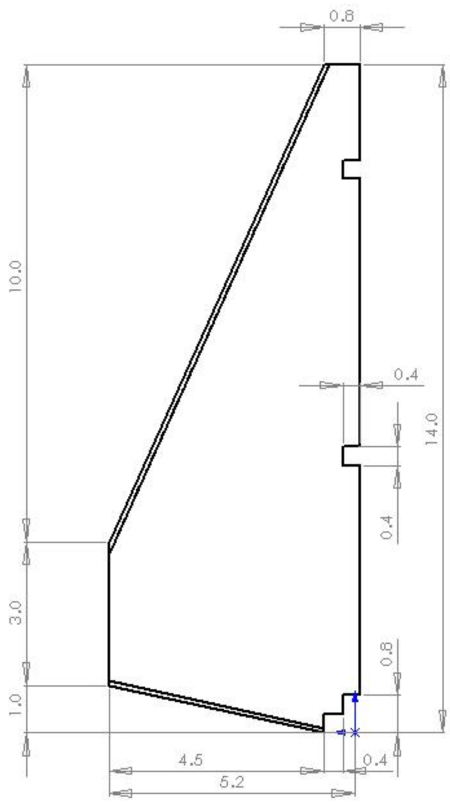

Figure 9 Fin profile. All dimensions are in inches.

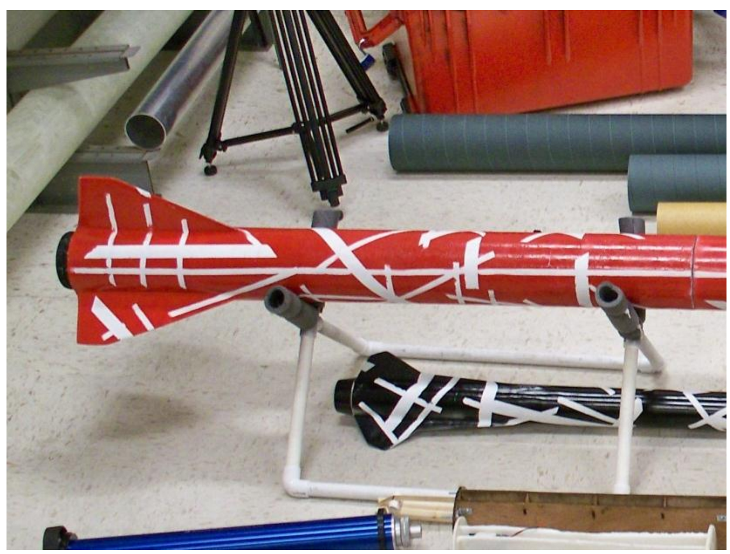

Figure 10 Completed booster section with fins.

Electronics

The Avionics bay of the vehicle is located in the center of the sustainer. Mounted on the outside of the hatch are the two key switches for the flight computers. The wiring of the key switches are connected between the battery and flight computers by a pair of JST connectors. This allows the key switches to be fully detached and the avionics to be removed without any rewiring. The disassembled avionics bay can be seen in Fig. 11 below.

The primary structure of the avionics bay is provided by two ¼” all-thread rods extending through both ends of the bay. Mounted on the all-thread are 1/8” panels of polycarbonate. These panels are bolted together with standoffs and lock washers. This assembly forms the electronics sled. Batteries are secured by zip-ties oriented laterally and horizontally. The flight computers are mounted by standoffs and screwed in to position.

Wiring for the ejection charges pass through holes in the bulkheads on either side of the electronics sled. There are four of these wiring tunnels, with two on either end of the bay. The wiring for the ejection charges passes through these and is connected to three terminal blocks on both sides of the avionics bay.

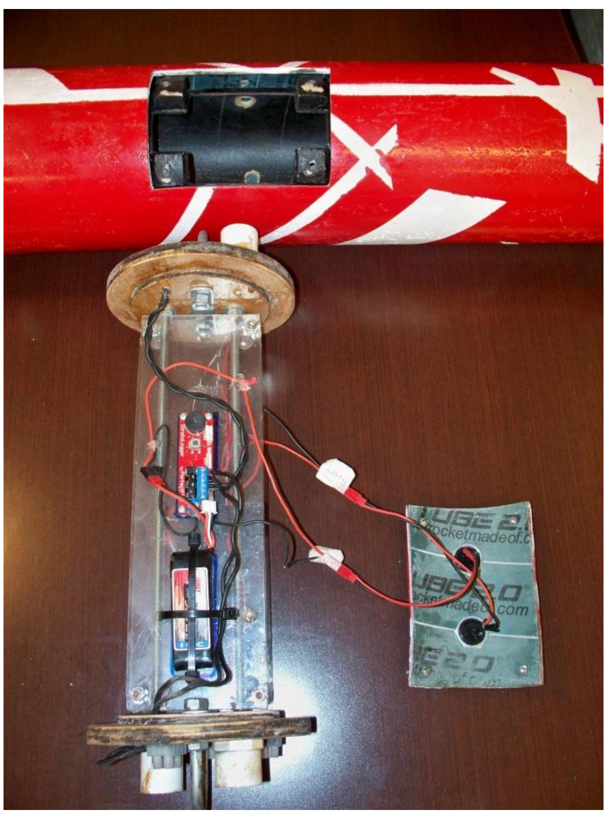

Figure 11 Disassembled avionics bay with bulkheads and hatch.

Figure 12 Bulkhead with ejection charge wiring connected to terminal blocks.

3.1.2 Flight Reliability

A successful mission includes launch, recovery, and deployment of the scientific payload. Confidence in the reliability of the vehicle is very high. It is expected to meet the mission requirements. The vehicle will be able to withstand flight loadings and the recovery events.

The objective of reaching as close to 5280 feet AGL as possible can be met by the vehicle. The motor chosen for the flight is capable of delivering more than the necessary total impulse to deliver the payload to this altitude. By knowing the drag characteristics the apogee can be adjusted by adding ballast.

Recovery of the vehicle in re-flyable condition is assured after ground testing and the flight test. The drogue parachute and payload have been shown to deploy from the vehicle after the apogee charges are fired. Shear pins keep the nosecone attached and the main parachute undeployed until the ejection charges are triggered. Ejection charge testing and the test flight have shown the robustness of the recovery system.

3.1.3 Test Data and Analysis

The recovery system was the most thoroughly tested part of the vehicle. In order to select the shear pins the forces acting to separate the vehicle prematurely must be analyzed. The pressure difference from ground to apogee will be 2.3 PSI and the area of the bulkheads is 22 square inches. So, the air pressure difference will exert a force of 52 lbs. toward separation even without the ejection charges if unvented. The weight of the vehicle and acceleration would contribute to around a total of 87.5 lbs. and selecting for three shear pins, the force each has to resist is 29 lbs. For this purpose, Nylon 6/6 2-56 screws with minimum shear strength of 31 lbs. were selected. Through ejection charge testing it was determined that a charge of 4 oz was desired for the primary charges of the main and apogee. A 2 oz charge only separates the nosecone to 4 feet, while the 4 oz charge separates it to 15 feet. The minimum charge necessary was deemed to be 4 oz and so the secondary charges were sized 50% larger to 6 oz of black powder.

Figure 13 Ejection with 2 oz charge and 5 foot separation.

Figure 14 Ejection with 4 oz charge and 15 foot separation.

3.1.4 Safety and Failure Analysis

A general assessment of risks, associated consequences and precautionary measures are enumerated in Table 1 as follows.

Table 1 Description of vehicle failure modes and risk mitigations.

Failure Modes	Causes	Effects	Mitigation
Airframe Zippering	-Not enough energy dissipated in shock cord. -High deployment velocity	-No longer flyable rocket	-50 foot Shock Cords
Fin Shearing	-Excessive aerodynamic loading. -Impact with launch rail.	-Unstable flight -Unsafe trajectory	-Fiberglass reinforced fins. -Epoxied rail buttons -Subsonic flight
Hang Fire	-Failure of motor to attain operating pressure or burn after ignition.	-Potentially live motor that is unspent -No launch	-Wait 10 minutes -Fix new igniter and reattempt launch.
Rail Buttons Let Go	-Twisting during launch -Catching on rail	-Non-vertical trajectory	-Straight fins -Aligned rail extension
Motor CATO	-Over pressurization of casing	-Destruction of casing and motor mount tube	-Maintain safe distance during launch. -Minimize personnel near vehicle while being primed
Over stability	-CG too far forward	-Non-vertical trajectory -Flight in to the wind	-Properly sized fins -Payload near to center of gravity
Coning	-Fins failing to provide corrective force -Off center CG	-Increased drag	-Maintain minimum stability.

3.1.5 Sub-Scale Test Results

A subscale rocket was constructed in order to gain proficiency at rocket construction, testing, and launch procedures. Construction of the subscale involved exclusively the use of fiberglass. Practice with using fiberglass turned out to be critical when fabricating parts for the full-scale vehicle. Critical techniques practiced involved fin alignment and mounting, fixing motor mounts, wiring of avionics, and the use of key switches. Lessons learned from testing involved in the subscale also transferred over to the full-scale. Specifically, ejection charge sizing and parachute packing for proper deployment.

Similar to the full-scale, the vehicle was modeled in OpenRocket. The model of the vehicle was improved by measuring the mass of each component and importing them in to the model. The vehicle was then flown on an I600R motor. The predicted altitude was 3619 feet. The model and flight predictions can be seen in Fig. 15 below.

Rocket Design

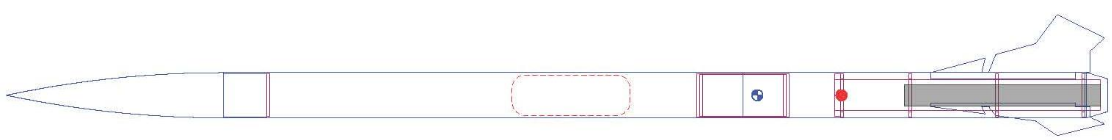

Rocket
Stages: 1
Mass (with motor): 7.14 lb
Stability: 1.86 cal
CG: 52 in
CP: 57.8 in

Altitude	3619 ft
Flight Time	274 s
Time to Apogee	14.1 s
Velocity off Pad	159 ft/s
Max Velocity	612 ft/s
Velocity at Deployment	38 ft/s
Landing Velocity	14.4 ft/s

Motor	Avg Thrust	Burn Time	Max Thrust	Total Impulse	Thrust to Wt	Propellant Wt	Size
I600R	572 N	1.12 s	818 N	640 Ns	18.00:1	0.71 lb	38/345 mm

Figure 15 Subscale model and flight predictions.

The subscale rocket was successfully flown on the I600R motor and recovered using a Perfectflite Stratologger altimeter. According to the flight computer, the motor took the subscale to 3651 feet AGL. This is a difference of 32 feet from the predicted altitude. This is less than a 1% difference from the actual to the predicted.

Such a close match is a validation of the modeling techniques used to predict the flight characteristics. A graph of the data recorded from the subscale vehicle's flight computer is shown in Figure 17.

Figure 16 Lift off of subscale rocket.

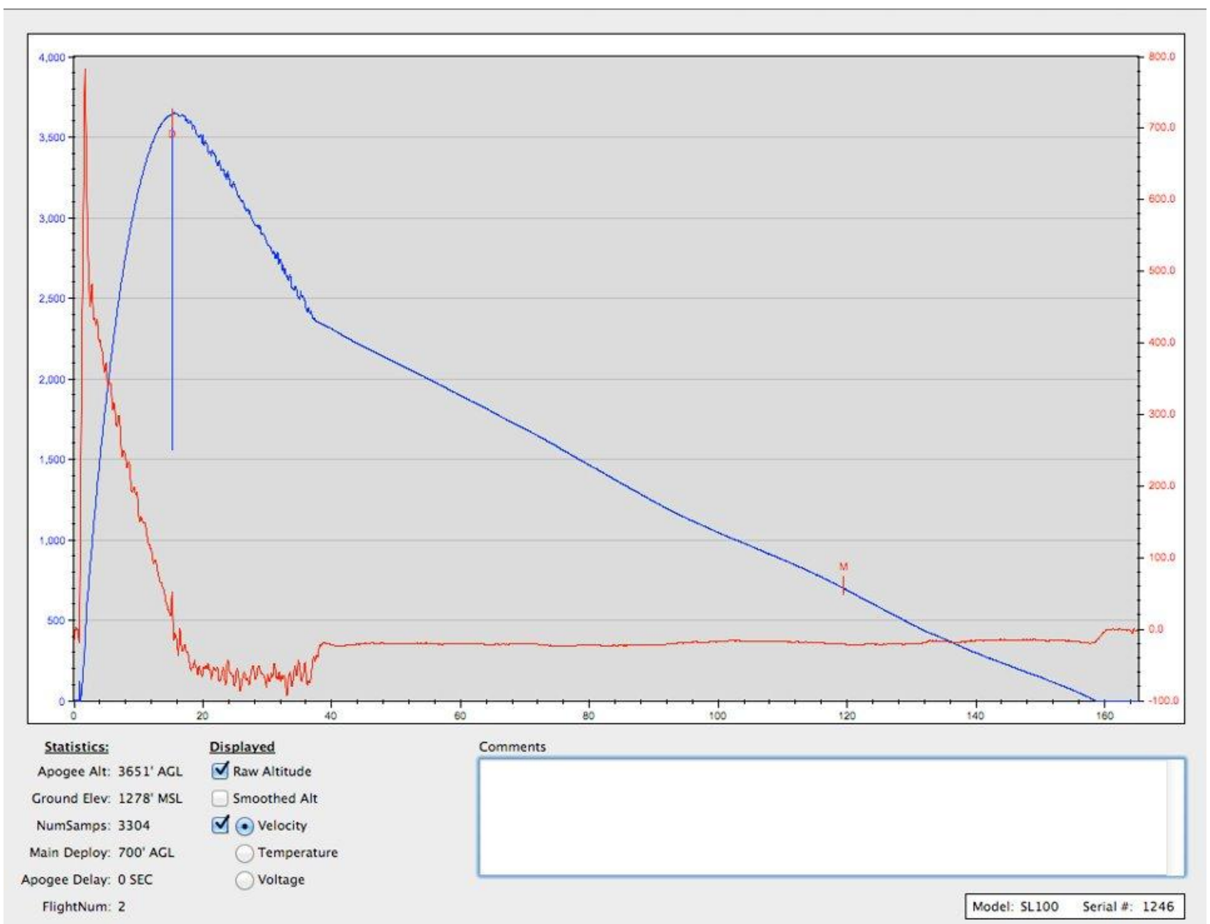

Figure 17 Data recorded from subscale flight.

3.1.6 Full-Scale Test Results

To begin with, the weather and obtaining a motor to launch on were the greatest issues encountered and delayed the full-scale test flight. The flight was performed on March 26th after the first attempt was scrubbed due to winds gusting at 36 MPH. Winds at the launch site in Pickrell, NE were an average of 6 MPH and were optimal for the launch.

Unfortunately, the motors that the team ordered did not arrive on time. The reason for this is that Aerotech was temporarily unable to ship hazardous material. So, our motors weren't shipped and will instead be transferred to the team by Off We Go Rocketry while in Huntsville.

With this deficit in available motors, it became necessary to find an alternative. Luckily, the members of the local rocketry club, THOR, were able to help the team out and provide an alternative motor. So, the test launch was performed on a 54mm CTI L730. The required adapter from 98mm to 54mm was also provided.

The recovery events included separation at the middle of the vehicle to deploy the drogue parachute and deployment but the payload remains tethered with its parafoil bundled. The secondary charge for the apogee separation was set fire 1 second later. The main charge is to separate the nosecone at 1000 feet AGL and deploy the main parachute. The secondary charge for the main detonates at 900 feet AGL. Then the parafoil was to be released and the vehicle to become untethered after detonation of a dual deployment link.

The configuration for this test flight included 5.5 lbs of payload and a gross lift off weight of 34.2 pounds. So a thrust to weight ratio of 4.84:1 was expected with this motor. Initial simulations in OpenRocket with the L730 Motor indicated the apogee of this launch to be at an altitude of 3592 feet AGL. The simulation data can be seen in Figure 18.

Altitude	3592 ft
Flight Time	136 s
Time to Apogee	15.7 s
Velocity off Pad	85.2 ft/s
Max Velocity	457 ft/s
Velocity at Deployment	69.8 ft/s
Landing Velocity	16.1 ft/s

Motor	Avg Thrust	Burn Time	Max Thrust	Total Impulse	Thrust to Wt	Propellant Wt	Size
L730	738 N	3.74 s	1217 N	2764 Ns	4.84:1	2.98 lb	54/649 mm

Figure 18 Full-Scale launch on the L730 simulation summary.

According to the Perfectflite Stratologger altimeter, our primary altimeter, the altitude reached by the vehicle was 3341 feet AGL. The secondary Raven2 altimeter recorded a very similar 3339 feet AGL. Both values are based on barometric pressures. The close agreement of the two altimeters shows that they are similarly calibrated and have been deemed reliable because of the small difference of two feet. The data from the Primary altimeter is graphed in Figure 19 and the secondary altimeter in Figure 20 on the following page.

Between the simulation and the recorded altitude there is an altitude difference of 250 feet. This is a 7.5% error of the actual from the predicted altitude. The most likely reasons for this discrepancy have been found to be the surface roughness of the vehicle and the angle of the launch rail. By refining the model of the vehicle to account for the surface roughness of the paint and increasing the launch angle of the simulation to 5 degrees, the predicted altitude is 3351 feet AGL. The percent error in the refined simulation is reduced to less than 1%. These changes to the model seem reasonable given the roughness of the paint and the uncertainty of the launch rail's angle.

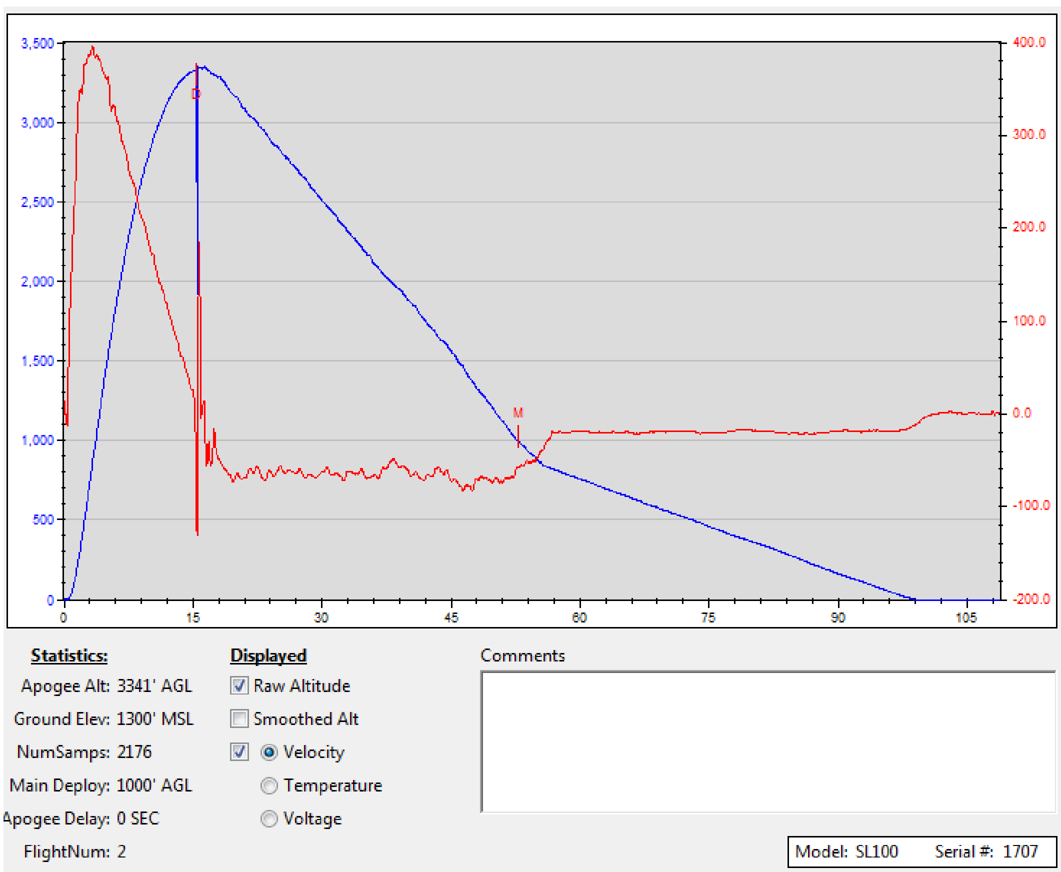

Figure 19 Perfectflite Stratologger primary altimeter altitude and velocity data.

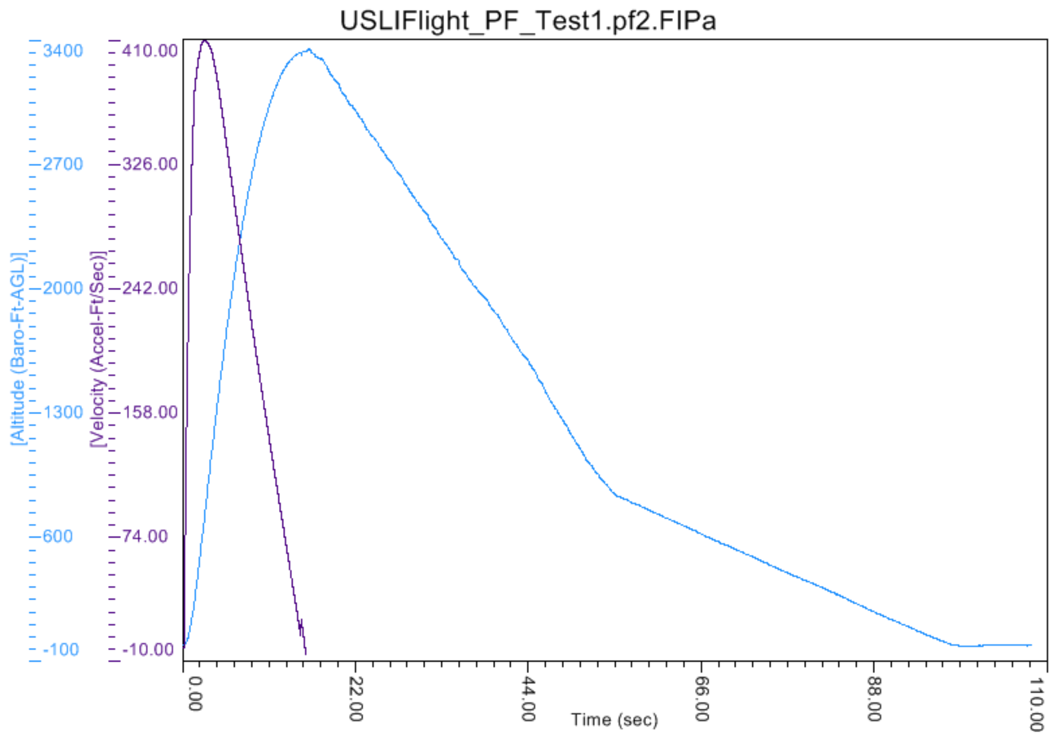

Figure 20 Raven2 Secondary altimeter altitude and velocity data.

3.1.7 Mass Report

Components and sections of the vehicle have been weighed for the total mass calculation, coming out to 23.7 pounds mass. These measurements were performed with a digital scale to the nearest tenth of an ounce and are listed in Table 5 below. The total vehicle mass previously estimated using the OpenRocket simulation software was about 27 pounds. Several components, notable the body tubes, came out to be less dense than what was modeled in the software even after reinforcement. The OpenRocket model was originally used to predict the mass of the vehicle and motor selection. A full listing of components used in this prediction is provided in the appendix. Comparing this prediction to the weights of actual components it can be seen that the estimate erred on the high side. This was done to ensure a powerful enough motor was selected. Not included in actual measurements are the motor mass, which is given, and the actual nosecone mass because it is still being shipped. It is not expected for the lift off mass of the vehicle to increase beyond 44.2 pounds mass and it is expected that up to 4.5 pounds of ballast may need to be added.

Table 2 Table of measured and predicted vehicle section masses.

Section	Component	Weight
Nosecone	Structure + Hardware (Estimated)	4lb
Sustainer	Structure + avionics bay	7lb 9.8 oz
	Drogue + shockcord	1lb 11.2 oz
	Main Parachute + shockcord	2lb 15.2 oz
Booster	Structure + MMT + Fins + Adapter	7lb 13.8 oz
	Sub Total:	23.76 lb
Other Components		
	Motor Hardware	4lb 13.3 oz
	Propellant	6lb 2.7 oz
	Payload(5lb) + Ballast	9lb 8 oz
	SubTotal:	20.5 lb
	Lift Off Total:	44.26 lb

3.2 Recovery Subsystem

3.2.1 As Built Recovery Subsystem

The selection of recovery subsystems components depends on the mass of the vehicle and deployment scheme. The mass of the vehicle with the payload is more important for the drogue parachute but also critical for the main parachute if the payload doesn't separate. The deployment scheme chosen for this mission is a dual deployment.

1) A 3' Drogue Parachute(77.9 FPS) will be deployed upon reaching apogee.
2) The Payload will be drawn out of the vehicle by the Drogue.
3) The vehicle will descend under the drogue until 1000-Feet AGL and will then deploy a larger Main Parachute(18 FPS) from the forward bay.

The attachment scheme for the recovery systems is well defined. All vehicle components will be tethered and the payload will be tethered until deployed independently. A listing of the major recovery subsystem components are shown in the table below:

Table 3 Major components of recovery subsystem

Component	Characteristic Dimension	Comment
Main Parachute	108”	18FPS -Hemispherical with 24” Spill hole
Drogue	36”	77.9 FPS - Mach 1 Ballistic X-Form
Shock Cord	52’ Main / 50’ Drogue	4200lb test - 1” Tubular Nylon
Wadding	24”	2 x Fire resistant protective cloth
Quick Links	¼” diameter	880lb rated Stainless Steel

Structural Elements

Loads will be transferred through the shock cord, recovery hard points, all thread connecting the avionics bulkheads and motor thrust ring. Under powered flight, the motor will provide thrust that is transferred to the vehicle at the aft motor retainer, and all the way to the nosecone through the airframe shell. This is kept centered by the coupler tubes between the Booster, Sustainer, and Nosecone.

During descent and after apogee, the load will be transferred through the 4200lb test 1inch tubular nylon shock cord to the drogue parachute near the middle connected by a ¼” 880lb rated quick link. At either end of the drogue shock cord are additional ¼” 880lb rated quick links. At one side this shock cord is attached at the 5/16” forged eye-bolt in the engine block of the booster and the opposite holds the sustainer at a ¼” U-bolt at the bottom of the avionics bay. Load is transferred through the avionics bay by two steel all-thread rods and to the still attached nosecone through the shear pins.
After the main parachute deploys, the load is transferred through the avionics bay by the two rods of ¼" all-thread to the ¼” U-bolt at the top of the avionics bay, through the

shock cord attached to the main parachute at one end with the main parachute at the base of the nosecone.

The use of swivel link on the main parachute will decrease the likely hood of tangling the parachute lines. Quick links on the parachutes and self-tightening figure-8 knots connecting the hard points elsewhere will form solid connections. The recovery system hard points are reinforced with washers on eyebolts and backing plates on the U-bolts against fiberglass reinforced bulkheads.

The engine block at the top of the motor mount tube is composed of a half inch bulkhead reinforced with four layers of 8 oz. fiberglass at either side. The top of this is cemented and reinforced even more with a quarter inch thick layer of resin on top that is bonded to the engine block, parachute eyebolt, and interior of the airframe. The Avionics bay bulkheads and nosecone bulkhead are similarly constructed from 0.6 of plywood and reinforced with 4 oz. fiberglass. The bulkheads are kept centered with one layer of plywood fitting into the couplers. This resists the tendency of the nosecone bulkhead to be skew off center after ejection of the main parachute.

Figure 21 Layout of recovery hardware from left to right:

(Engine Block) Eye-bolt+Quicklink, 50' Shockcord, Quicklink+3' Drogue, Quicklink+U-Bolt, all-thread(Avionics Bay), U-bolt+Quicklink, 52' Shockcord, Quicklink+U-bolt (Nosecone)

Electrical Elements

The flight computers being used for the vehicle are the Perfectflite Stratologger and the Featherweight Raven2 Altimeter. The Stratologger has been selected as the primary flight computer for officially reporting the flight altitude. The main difference between the two is that the Raven2 possesses a total of four pyro outputs while the Stratologger only has two. A wiring Diagram of the avionics bay is provided in Figure 22 below.

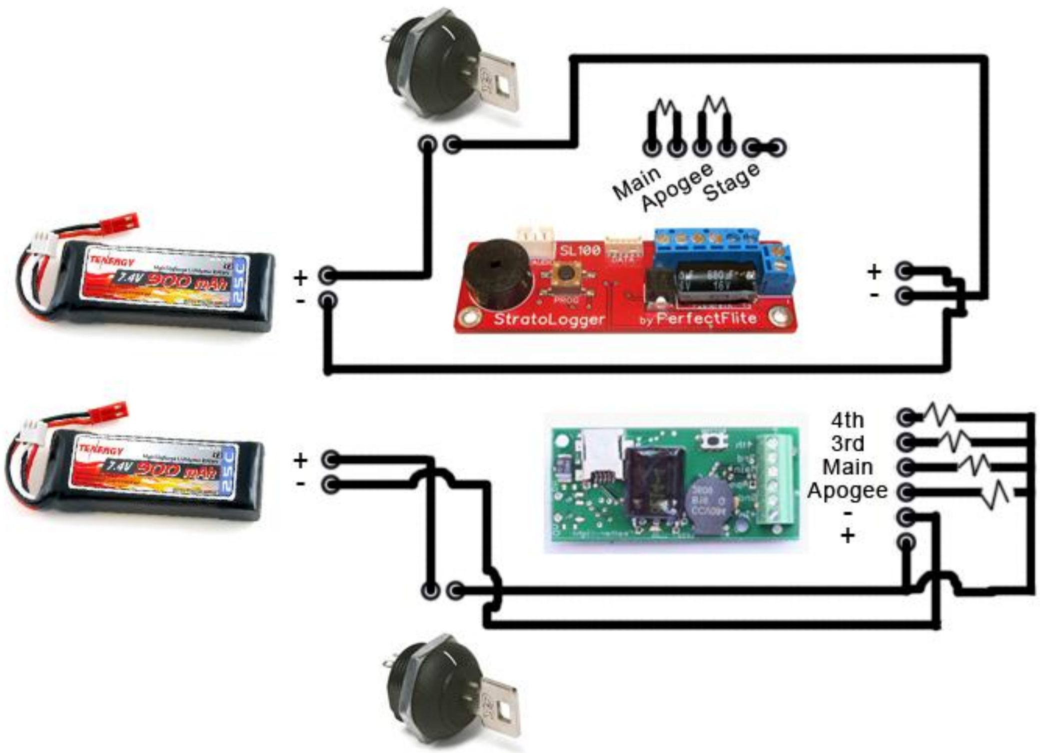

Figure 22 Wiring diagram of avionics bay showing how the key switches are integrated in the circuit.

Power for each flight computers is provided by two independent Tenergy 900mah 7.4v lithium polymer batteries. The batteries have been shown to power the flight computers in standby mode for longer than 4 hours and both measured a voltage drop of less than 0.1 volts after the test flight. These batteries terminate in male JST connectors. In between the batteries and flight computers are the key switches. The leads of the key switches also terminate in male JST connectors. The batteries and key switches are connected to the flight computers by two female JST connectors. This setup allows the batteries to be disconnected for easy recharging and the key switches to be removed for disassembling the avionics bay. The avionics bay hatch will allow the flight computers to be activated from outside the vehicle by way of key switches

The flight computers will have an interface between both the upper and lower avionics bay bulkheads as well as to the exterior of the vehicle through a removable hatch or panel. At either avionics bay bulkhead, there are three wiring terminals allowing both computers to be connected to a primary charge and the Raven2 to a secondary ejection charge. This allows for the Raven2 to have double redundancy and be redundant with the Stratologger on the primary charges. A block diagram of the computer connections is provided in Figure 23.

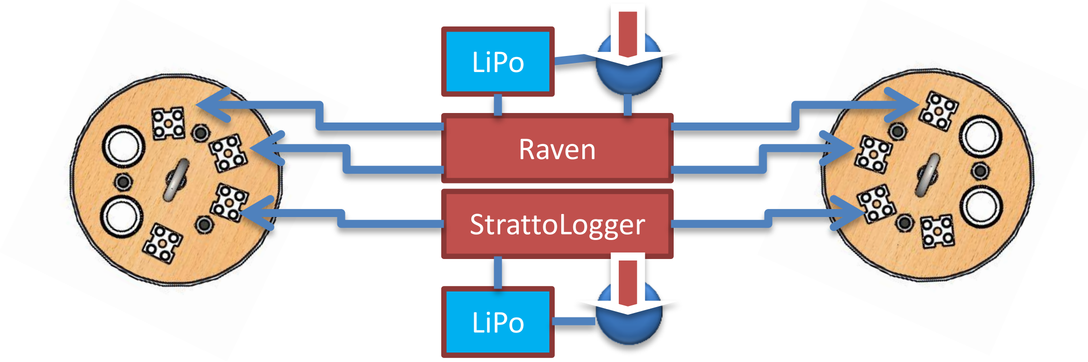

Figure 23 Block Diagram of Avionics connections.

Rocket Locating Transmitters

The locating transmitter of the rocket itself has been changed from a BRB900 to a First Person Video package with integrated Eagle Tree Systems GPS. The transmitter for this system transmits at 2.4 GHz at a power of 500 mW. The range of this system is about 1.5 miles line of sight with the 12 dB patch antenna with a 35 degree beam width. This is extended by using a diversity controller to instead receive from a 14 dB gain Yagi antenna with an 18 degree beam width. The maximum distance of the Yagi antenna hasn't been tested. The transmitter hasn't been shown to affect the operation of the flight computers in any way even with long e-matches connected.

This system is located in the nosecone of the rocket and is mounted on a polycarbonate electronics sled. The transmitter is outfitted with its own cooling fan and a hole is cut near the base of the nosecone for the camera to peer out from. Video from this transmitter is overlayed with GPS, altitude, g-forces, battery voltage and transmitter temperature.

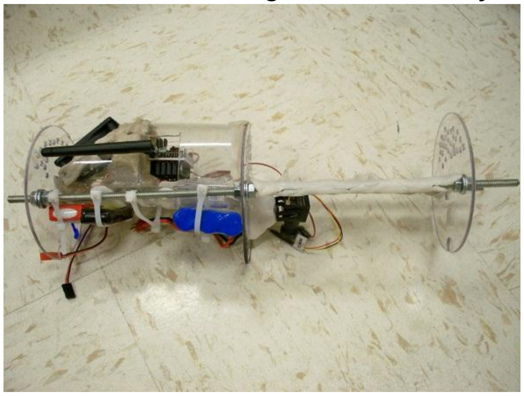

Figure 24 First Person Video transmitter with Eagle Tree Systems GPS and sensors.

3.3 Mission Performance Predictions

3.3.1 Mission Performance Criteria

Criteria for a successful mission are as follows: The launch vehicle must reach an altitude of 5,280-Feet above ground level, use a dual deployment recovery system, deploy a payload on demand, and recover all components in a re-launch able condition.

3.3.2 Simulation Data

What follows are the dimensions and models used in OpenRocket simulations. After the test flight, the drag characteristics of the vehicle were accounted for by increasing the surface roughness in the model. Predicted weights have been updated with actual weights and are tabulated in the appendix. The motor used in the simulation is an Aerotech L1170 FJ. This motor can deliver the vehicle and a 5 pound payload to the target altitude. The Propellant used is the Fast Jack formulation of APCP. Additionally, a secondary motor and tertiary motor option will be on hand if this ultimately proves insufficient for the payload mass.

Rocket Design

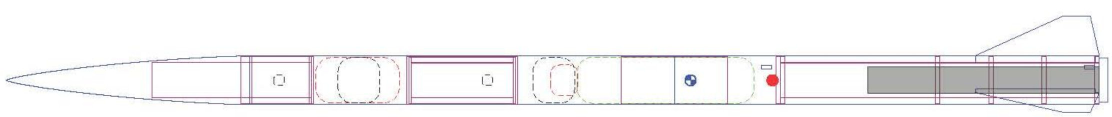

Deimos
Stages: 1
Mass (with motor): 39.8 lb
Stability: 1.68 cal
CG: 77.3 in
CP: 86.6 in

Figure 25 OpenRocket model of vehicle with selected motor and 5.0lb payload.

Table 4 Candidate motor evaluated in simulation.

L1170FJ-P

Altitude	5305 ft
Flight Time	157 s
Time to Apogee	18.2 s
Velocity off Pad	84.3 ft/s
Max Velocity	655 ft/s
Velocity at Deployment	72.4 ft/s
Landing Velocity	16.7 ft/s

Motor	Avg Thrust	Burn Time	Max Thrust	Total Impulse	Thrust to Wt	Propellant Wt	Size
L1170FJ	1207 N	3.49 s	1473 N	4214 Ns	6.82:1	6.17 lb	75/665 mm

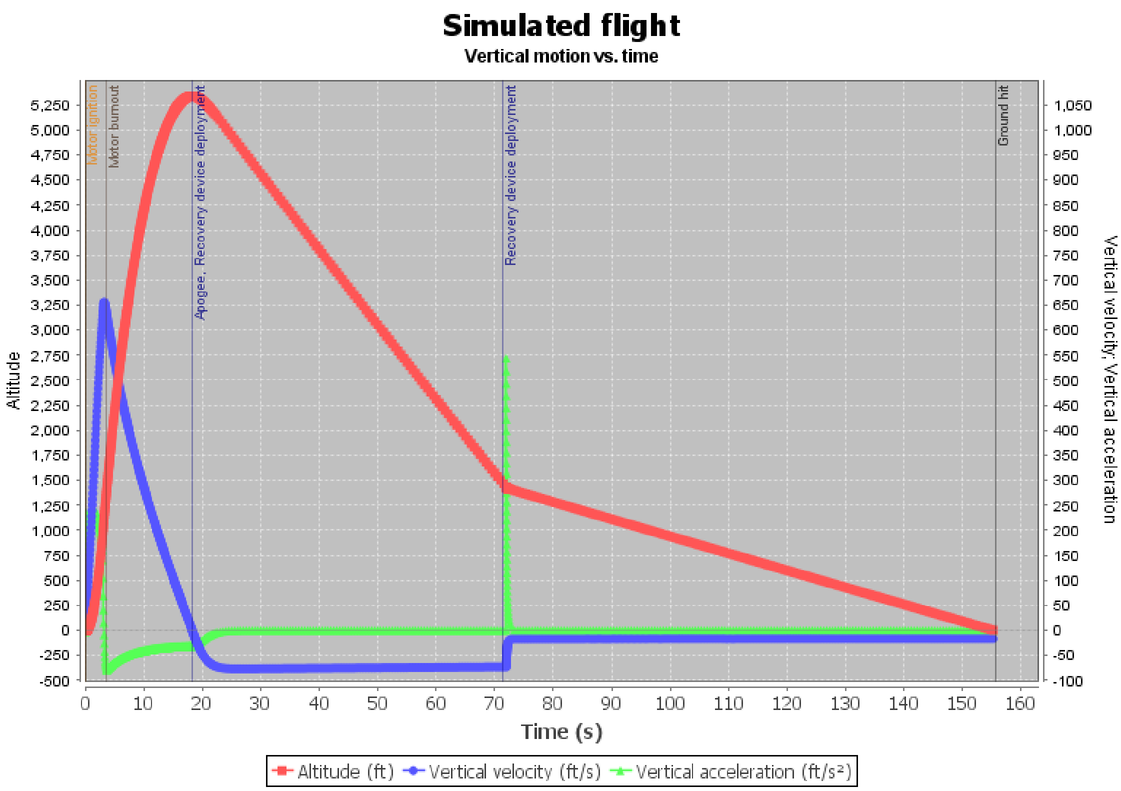

Figure 26 Vertical motion vs. Time. (Altitude, Velocity, Acceleration)

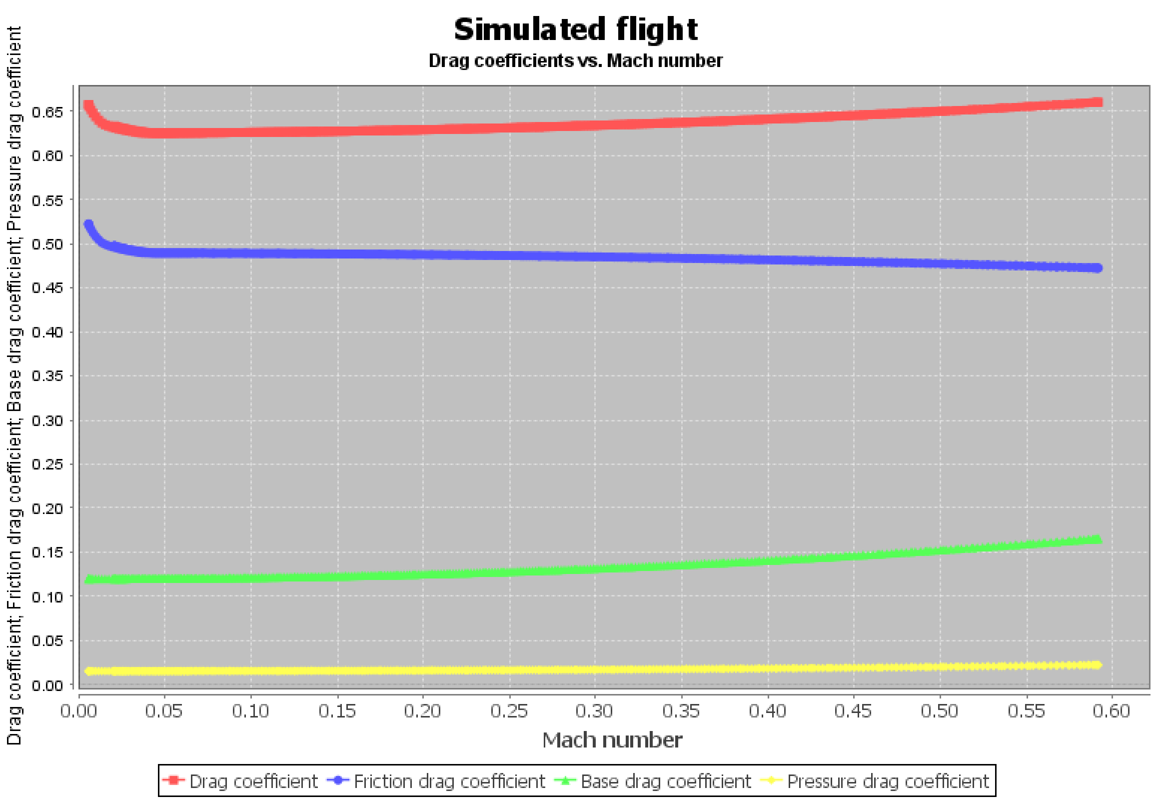

Figure 27 Drag coefficient of vehicle up to expected mach number.

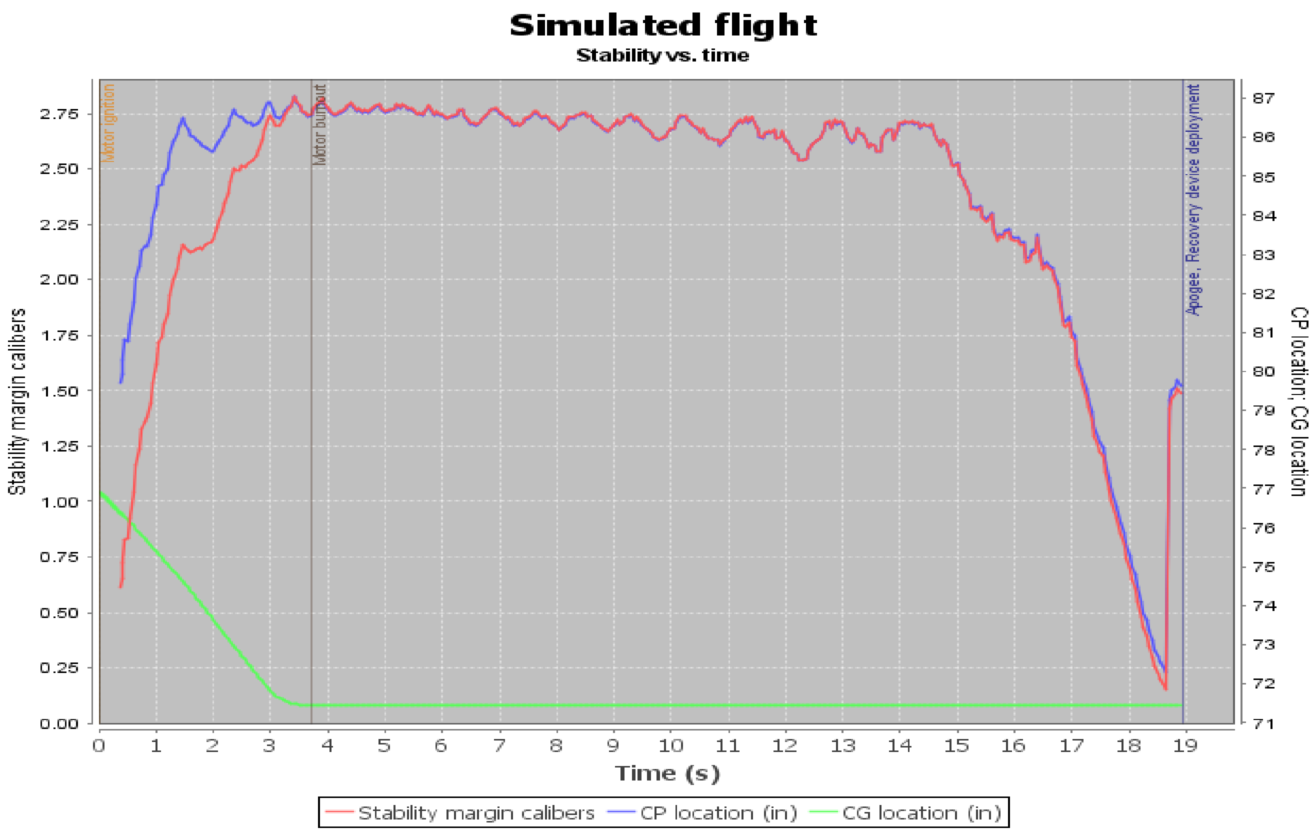

Figure 28 Stability margin of vehicle throughout flight.

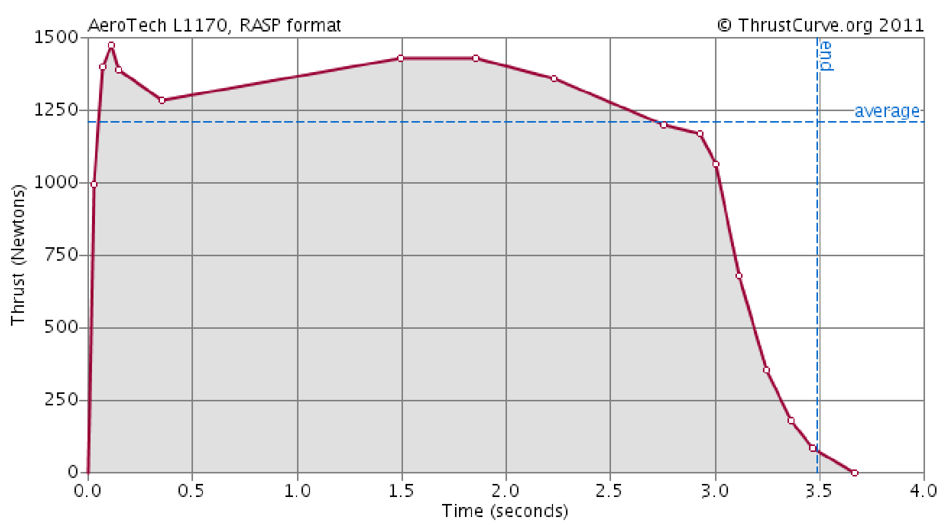

Figure 29 Motor Thrust Curve

The conclusion drawn from this simulation is that given the updated drag characteristics the L-1170 FJ motor may have enough impulse for the mission at hand. So, in order to reach the altitude goal, either the secondary or backup motors may need to be used. Although, the drag characteristics of the vehicle may be improved by sanding the paint, it may be wiser to accept the drag characteristics as they are and use one of the motors that work with this.

With the new data, it is shown that the total drag coefficient of the vehicle increases to about 0.67 throughout the flight for this simulation. This is an average increase in the drag coefficient of 0.17 and the largest contribution to drag is still from skin friction. The base drag could be reduced by adding a boat tail to the rear of the vehicle but advantages would be reduced by the resulting increase in surface area and the reduction in stability. Larger fins would be needed in that case because the boat tail would shift the center of pressure forward. It can also be seen that the vehicle maintains a fair margin of stability all the way through the ascent of the flight.

The vehicle design seems suitable as is with this motor so long as the payload doesn't increase in mass. If it becomes apparent that the vehicle does require a greater impulse motor, then the secondary L1420R or tertiary L1300R motors that are available will be selected. An addendum with the updated simulations will be submitted if this is the case. Otherwise, the vehicle will be flown on the currently selected motor in April.

Descent Energy

The descent energy of the vehicle has been calculated under projected descent rates after apogee in three sections and after main deployment in four sections. Most importantly, the descent energies at landing are below the limit of 75 foot-pounds force. The deployment main deployment velocity has been reduced to below 100 FPS and the landing velocity is still under 20 FPS. These calculations are tabulated in Table 7.

Table 5 Descent energy calculations with simulation descent speeds and measured section weights.

Event	Section		weight (lbf)	Speed(ft/s)	Energy (ft-lbf)
Apogee	1	Nosecone + Sustainer	10.6	77.9	998.8
	2	Booster	12.6	77.9	1187.3
	3	UAV(Tethered)	9.5	77.9	895.2
Main 1000'	1	Nosecone	4	18	20.1
	2	Sustainer	6.6	18	33.2
	3	Booster	12.6	18	63.4
	4	UAV(Released)	9.5	5	3.7

Drift Calculations

Dual deployment of the parachutes will reduce descent time and therefore drift of the vehicle from the launch pad after apogee. By launching slightly in to the wind the drift distance may also be reduced at the cost of altitude. Calculations involved in drift assume that wind speed is the same at all altitudes. By reducing the altitude at which the main parachute is ejected it can be shown that drift from the pad may be reduced, for the range of wind speeds in question, to fall within the limit of half a mile from the pad. Notably, at 20MPH wind conditions it is necessary to reduce the main deployment to 500 feet AGL to reduce drift sufficiently.

Table 6 Tabulated drift calculations

DescentTime (s)	Wind Speed(MPH)	(Ft/s)	Drift Distance(ft
(1000' Deployment)			
108.1	0	0	0
108.1	5	7.3	792.7333
108.1	10	14.6	1585.467
108.1	15	22	2378.2
(500' Deployment)			
88.1	20	29.3	2584.267

Proper mitigation of drift in 20 MPH winds with a 2MPH variance is also supported by the OpenRocket simulation with the vehicle launching with a 1 degree inclination in to the winds. The vehicle is predicted to land within half a mile of the launch pad with both methods.

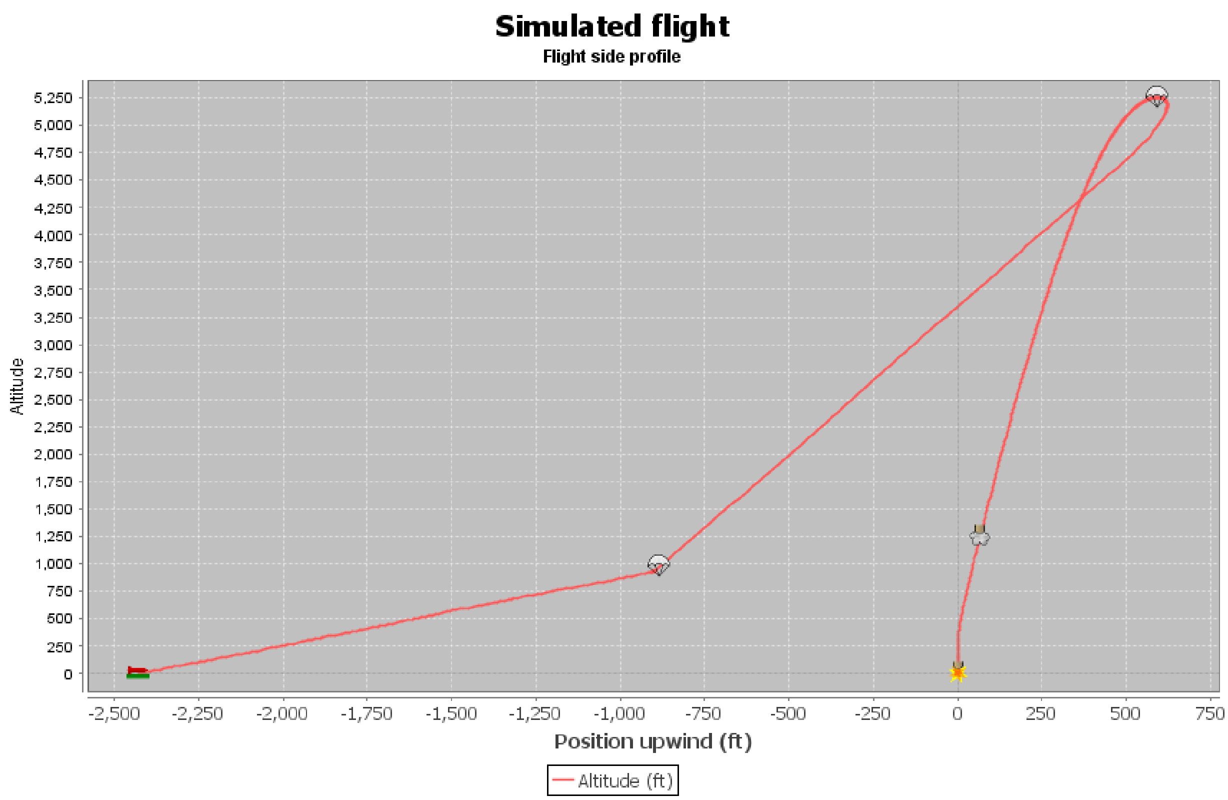

Figure 30 OpenRocket simulation drift data in 20MPH winds.

3.4 Verification (Vehicle)

How the design requirements outlined in the USLI Handbook are fulfilled by the project is listed below in Table 6. Also included is how fulfillment of the requirements is verified.

Table 7 Fulfillment of Competition Design Requirements.

Requirement	Fulfillment	Status
Scientific Payload	Experimental Ambient Wind Energy Scavenging System	Static test rig completed. Airframe constructed. Programing in progress.
Launch AGL	Careful calculations using OpenRocket simulations and adding necessary ballast to slightly over powered motor.	Design
Official Altimeter	PerfectFlight StrattoLogger	Integrated and tested for accuracy
Recovery	A subassembly is being used to separate the Avbay, as well as two key switches each having its own LiPo battery	Integrated and tested for reliability.
Magnetic shielding	Using a thin metal foil to shield components	Tested
Subsonic flight	Our simulations have shown that this will be far under supersonic flight	Analysis and Demonstration
Reusablility	Safe landing at low velocity with low impact energy.	Demonstrated at 18FPS test launch landing
Drogue-Main Parachute Recovery	Drogue to deploy at apogee. as well as a Main parachute to deploy at 1000ft to 700ft AGL	Design and demonstrated
Shear pins	Three 2-56 Nylon 6/6 screws to be used at each section.	Ejection charge testing completed.

Requirement	Fulfillment	Status
Tethered sections	We have 3 sections tethered together, Nosecone, Sustainer, Booster	Design/Construction
Launch Window	With proper pre-flight checklists we will use all minutes of the preflight time well	In our Possession, and practiced at test launches.
Rocket on Pad	All our components should last many hours on the pad, our batteries will last much more than a hour.	Battery life tested out to 4 hours.
Launching Vehicle	Ten second count down standard.	Standard for all launches
External launch circuitry	Only our motor will need external circuitry, which lies under the equipment needed to launch	Standard for all launches
Flight Data	We will have a person(s) that will collect the data after launch	Standard for all launches
Flight Tracking	We have an Eagle Tree Systems GPS tracking system with live video.	Range testing to 1.5 miles.
Rocket Motor	Motor in question is an Aerotech L1170 FJ-P	Motor selected by analysis
Rocket Motor Requirements	As stated above, it is a L class motor	Inspection. This motor has been certified
Full test launch	Planned for February with back up date in March	Performed in March

Requirement	Fulfillment	Status
Prohibited items	None of the listed items are in our rocket design	Inspection
CheckList	We have an extensive checklist we have used before, and will always use	Inspection
NAR Mentor	Tom Kernes	Inspection. He has done many flights and qualifies
Payment	Budget shows we will fall short of $5000 dollars on the launch pad.	Analysis.

3.5 Safety and Environment (Vehicle)

Safety Officer: Paul Kubitschek

Table 8 Vehicle failure modes and mitigations.

Possible Failure	Effect of Failure	Mitigation
Catastrophic explosion either on the pad or in flight	The possible destruction of the rocket and/or pad	Properly load motor by qualified personal
Fins shear off of airframe	Loss of stability crashing of vehicle is imminent	Proper fins should be constructed
Failure of airframe separation	Rocket comes down at high velocity, possible tumble, or nose dive	Make sure ejection charges are properly packed as well as shear pins
Parachute failure	Parachute becomes tangled in cords and possible destruction of vehicle	Properly load parachute in parachute bag and properly place in airframe with shock chords
Loss connection to radio tracker	Rocket may become lost	Make sure radio equipment is securely attached, charged and highly visible

Before construction the members of the team have read and reviewed the NAR safety codes. These safety guides give all the needed details for proper construction and operation of high power rockets. Safety in our team is very important and we take all precautionary measures to protect personnel from injury. Our team doesn't use many chemicals for our rocket as our motor is pre-made, but we do use other chemicals that release toxic fumes. For this we have a well-ventilated room (Large overhead Fume), as well as face masks.

In the field, the team will practice good safety procedures by maintaining a safe distance from launch pads and additional measures. The team will not go to recover components after launch until released to do so by the range safety officers. Working conditions in the field will be kept comfortable for the team by using canopies, and sufficient water supply. Additionally, communication will be maintained through walkie talkies.

3.6 Payload Integration

The basic requirements for integration include system initialization, fitting clearance, and place in main parachute bay loading order. As the Payload is a fully independent system it must be activated and powered by itself prior to loading. As the payload may expand beyond the bay’s diameter it must be locked in to a collapsed state to prevent interference during ejection. As it occupies the same bay as the main parachute there is a very specific order that must be followed when the payload is integrated with the launch vehicle. In short, the operations of integration are:

1) Powered on, systems initialized and communicating with ground station
2) Collapse wings in to undeployed state
3) Parafoil secured to payload airframe by dual deployment link and packed in deployment bag
4) Parafoil inserted in bay below drogue parachute
5) The payload airframe inserted below parafoil with enough clearance for shock cord to top of booster assembly
6) Booster section slid over payload and coupled to bottom of sustainer section
7) Shear pins inserted in to coupler between sustainer and booster sections.

Figure 31 Payload and payload prototype airframe with recovery hardware.

4.0 Payload Criteria

4.1 Selection, Design and Verification of Payload Experiment

4.1.1 System Level Overview

The deployable payload will be designed to separate fully from the rocket and descend under a parafoil. The structure will house an experimental energy scavenging system, which will autonomously activate shortly after separation and will collect and transmit data throughout descent. The relevant systems are as follows:

1) Airframe
2) Experimental ambient wind energy scavenging system

Payload Airframe Functional Requirements

Performance Characteristics:

The airframe must strong enough to be suspended from a parachute, stable during flight and fit within the launch vehicle. The payload airframe will be designed to house the experimental ambient wind energy scavenging system. The design must allow for the wind belts to be oriented in the direction the vehicle is traveling. It will be required to protect the required electronics during ejection from the launch vehicle, aerodynamic forces and impact at landing.

Options:

1) Horizontal Deployable Windbelt
2) Vertical Static Windbelt

Selection Rational:

The structural housing the payload electronics on bulkheads and parachute attachment is common between all considered options, but the method by which the windbelts are oriented is more variable. Thus, the criteria for selection involve maximizing the effectiveness of the windbelt system. This enables the experiment to be optimally performed. So, the option that allows the windbelts to be most easily oriented in to the wind will be chosen.

Selected Concept:

The selected concept is the Horizontal Deployable Windbelt. Having the windbelt mounted on a fold out wing allows greater control of the windbelt orientation. A vertically mounted windbelt would not be able to angle downward. The wing will be allowed to rotate around its hinge mounting. As the payload will be descending vertically and translating horizontally the vector of the incoming airstream will be directed up and to the rear of the payload. Thus, it is advantageous that the windbelt may be angled downward. The selected payload design can be seen in Fig. 32 below.

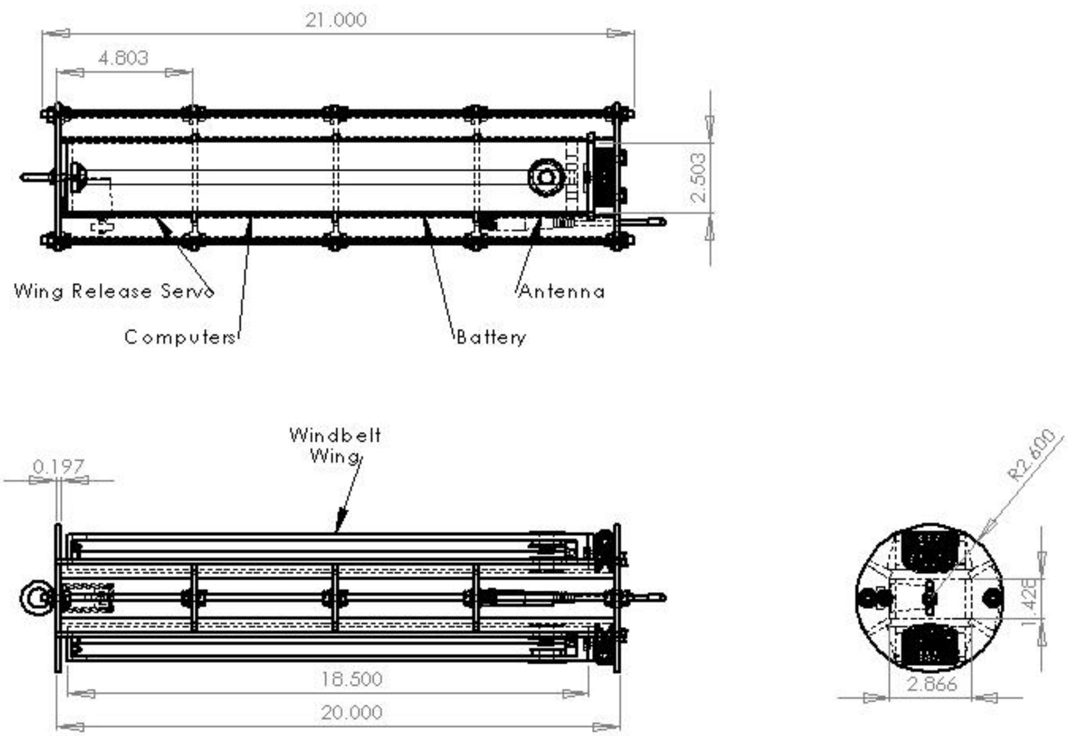

Figure 32 Selected Payload Design with deployable wings. All dimensions in inches.

Experimental Ambient Wind Energy Scavenging System Functional Requirements

The ambient wind energy scavenging system consists of two rigid wind structures that unfold outward from the main payload body shortly after the payload is deployed from the rocket (Fig. 34). Each wing structure supports a separate wind belt assembly (Fig. 33). This consists of a flexible ribbon with a permanent magnet attached to the ribbon at each side. During descent, the motion of the ribbon due to the wind moving past the wings causes the magnet to move relative to two copper coils. This induces a voltage in the coils in accordance with Faraday's Law.

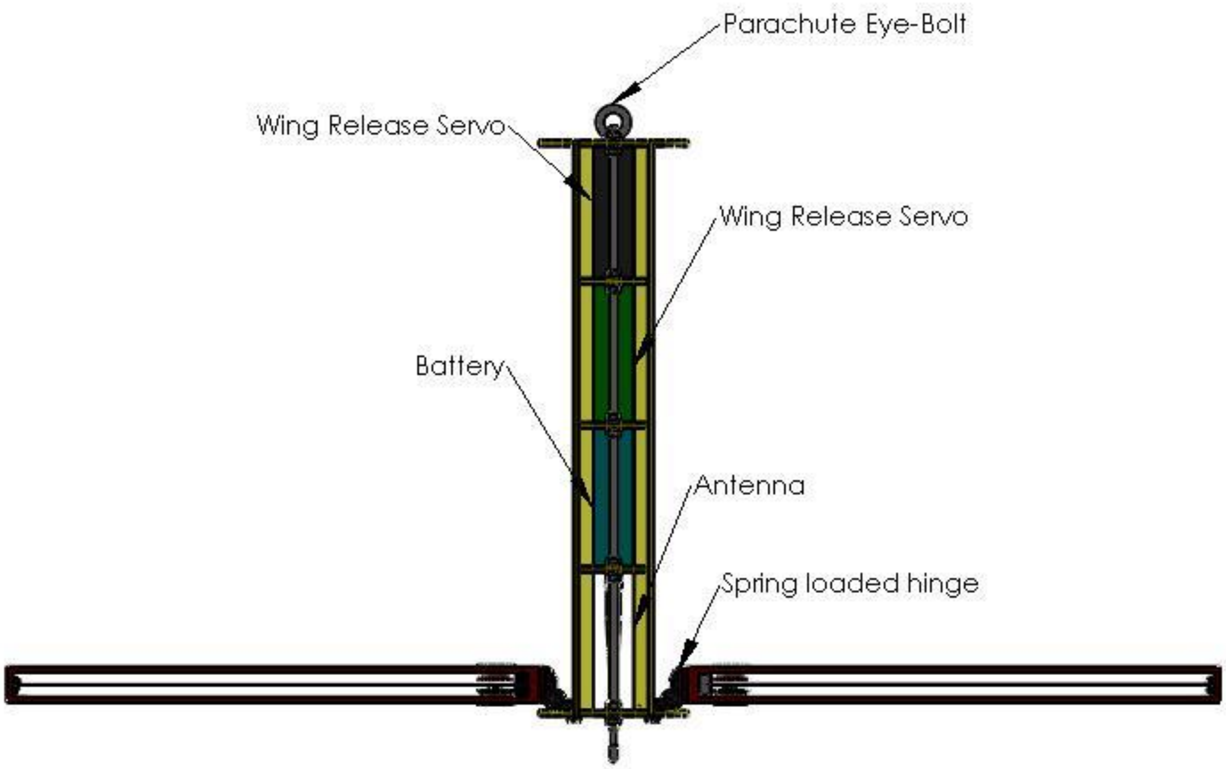

Figure 33 Deployed profile of payload and compartment assignments.

Figure 34 Wing structure with embedded windbelt assembly.

We propose that the power generated by a windbelt system is a function of the oscillation mode of the ribbon excited by the incident airflow. To investigate this, an active control system will be used to adjust the tension in *one* of the windbelts at regular intervals throughout descent. The other windbelt will serve to provide a baseline to which we will compare the performance of the primary windbelt. The belt tension required to optimize the windbelt motion for a measured wind speed will be determined through pre-flight tests.

Performance Characteristics:

The active belt tension control system will be required to autonomously adjust the tension in one of the windbelts beginning shortly after the wing structures are locked into place and terminating shortly before wing retraction. In addition, the magnitude of the voltage generated by each windbelt will be transmitted to the ground station computer every five seconds throughout this time period.

Subsystems:

The main subsystems necessary to accomplish the payload objective are as follows:

1) **Primary and secondary windbelt systems.** Each is supported by one of the wing assemblies that fold outward from the payload body shortly after separation from the rocket. Each windbelt system is identical and symmetric. The key components of this subsystem are as follows:

    a. Windbelts (taut membranes of mylar-coated taffeta)
    b. Permanent magnets
    c. Copper coils

    Evaluation and verification consists of demonstrating that a voltage is induced in each copper coil due to motion of the ribbon and magnet. This is determined by connecting the ends of each coil to an oscilloscope.

2) **Active windbelt tension control system.** This subsystem autonomously controls the tension in the primary windbelt in order to maintain a resonance condition with the incident airflow. The wind speed is read and the adjustment made every three seconds during the time that the wing structures are unfolded. The key components are as follows:

    a. Arduino Nano microcontroller
    b. Geared servo motor

    Evaluation and verification consists of demonstrating that the microcontroller can control the servo motor to loosen or tighten a belt based on an input wind speed and a hardcoded lookup table.

3) **Sensors and transmitter.** This subsystem provides information to the microcontroller about the wind speed, as well as acquires and transmits altitude

and GPS data to the ground station computer during flight. The key components are as follows:

a. Anemometer
b. Altimeter
c. GPS
d. Transmitter

Evaluation and verification consist of conducting benchtop tests of each sensor and comparing the acquired data to know values. The operation of the transmitter will be verified by attempting to transmit data over progressively longer distances.

4) **Power conversion system.** The voltage generated in the copper coils must be combined, rectified and smoothed before it is sent to the analog input of the microcontroller for measurement. This will be accomplished using a power conversion circuit board containing the following components:

a. Operational amplifier summing circuit
b. Full-wave rectifier and smoothing circuit

Each circuit will be verified individually before they are combined. The complete circuit will then be tested on a breadboard before the final version is transferred onto a PCB. Finally, the PCB will be tested before it is integrated into the remainder of the payload system. A basic block diagram of the power conversion system is shown in Fig. 35:

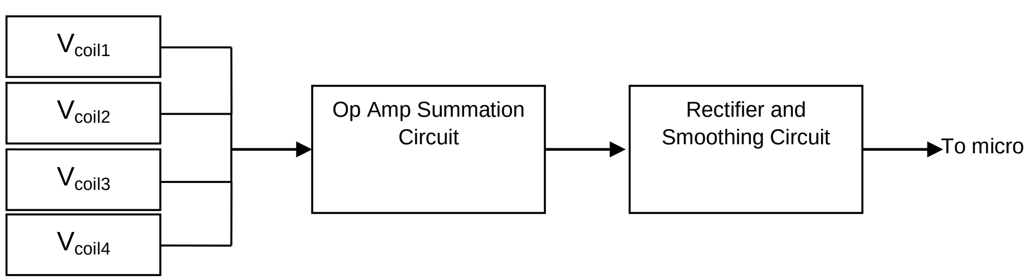

Figure 35 Block diagram of power conversion system.

The block diagram in Fig. 36 shows how the subsystems and key components will work together to achieve the payload objectives.

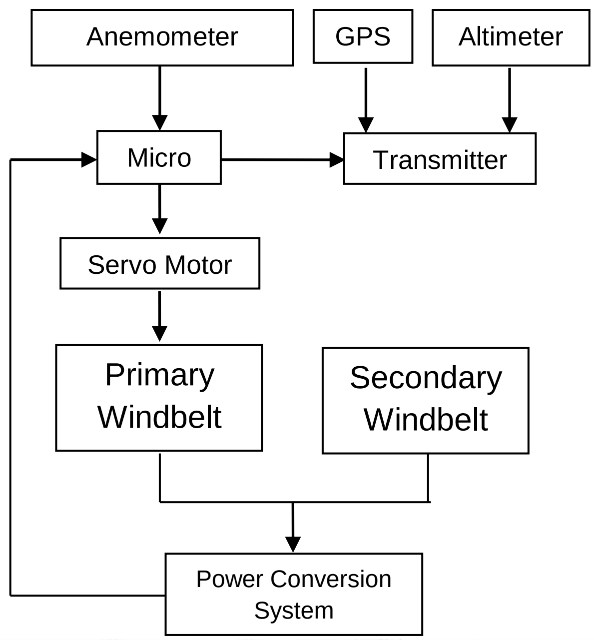

Figure 36 Interaction of subsystems and key components.

4.1.2 Verification Plan and Status

Table 1 Summary of verification plan.

Payload Requirement	Design Feature	Verification Method	Status
Payload deploys from rocket	Ejection charge	Testing	Test Launch =Successful
Payload parafoil deploys	Order of Parachute Packing	Testing	Test Launch = Needs to be moved
Wings unfold	Retractable Cable	Testing	Ground Test =Successful
Resonance	Active tension control	Testing/Analysis	Ground Test

condition maintained in primary windbelt	system		=Successful
Generated voltage transmitted every 5 seconds	Power Conversion & Transmitter System	Testing/Inspection	Ground Test =Programmed
GPS and Altitude data transmitted every 5 seconds	Sensor & Transmitter System	Testing/Inspection	Ground Test =Programmed
Wings retract	Retractable Cable	Testing	Pending

4.1.3 Preliminary Integration Plan

The basic requirements for integration include system initialization, fitting clearance, and place in main parachute bay loading order. As the Payload is a fully independent system it must be activated and powered by itself prior to loading. As the payload may expand beyond the bay's diameter it must be locked in to a collapsed state to prevent interference during ejection. As it occupies the same bay as the main parachute there is a very specific order that must be followed when the payload is integrated with the launch vehicle. In short, the operations of integration are:

1) Powered on, systems initialized and communicating with ground station
2) Collapse wings in to undeployed state
3) Parafoil secured to payload airframe and packed
4) Parafoil inserted in bay below main parachute
5) The payload airframe inserted below parafoil with enough clearance for shock cord to top of booster assembly
6) Booster section slid over payload and coupled to bottom of sustainer section
7) Shear pins inserted in to coupler between sustainer and booster sections.

4.1.4 Repeatability of Measurement

If this experiment were repeated several times, each collected dataset would be expected to vary greatly from one test to the next. This is because the generated voltage is a function of the wind speed encountered, and this is in turn dependent on environmental conditions. However, the general trend of the data would be expected to remain the same from one test to the next. For example, if it was determined in one experiment that the average generated power from the primary windbelt was significantly greater, about the same, or significantly less than the average generated power from the secondary windbelt, we would expect this general relationship to hold if the experiment was repeated.

4.1.5 Recovery System

The components of the recovery system simply include a parachute and the necessary hardware to attach it to the payload airframe. A Ram Air Parafoil was chosen to allow the payload to gain a horizontal velocity that would provide ample airspeed to feed the windbelt energy scavenging system. The parafoil being used is 2.1 meters in total span and can be seen in Figure 35 Below. The controllability of the parafoil does allow us to set the payload into a spiraling descent that would be advantageous for the mission.

The Parafoil is connected to a swivel link to an eye-bolt at the top center of the Payload Airframe. Before being released, the parafoil is packaged in to a deployment bag linked to the rocket. After release the payload will pull the parafoil from the bag and will automatically deploy. The release of this will use a dual deployment link that can be fired by sending a message to the ground station.

Figure 37 Parafoil for Payload measuring 2.1 meters.

Figure 38 L2 Tender Descender tethering payload.

The payload release has been changed from a servo actuated release to a dual deployment link. The product name of the dual deployment device is the L2 Tender Descender and is shown in Figure 38. This is rated to 2000lbf of shock load itself. This device is essentially an explosive bolt that keeps the parafoil packaged and the payload connected to the shock cord. The dual deployment link was selected because it was designed to handle high load deployment.

During the test launch, the deployment bag was not available and the parafoil was received that day. The team had to test and employ the deployment scheme for this on the same day. So the parafoil was packaged in a tightly wrapped flame protector. What worked with this is it kept the parafoil packaged until the dual deployment device fired. Unfortunately, the placement at the base of the drogue caused the lines of the parafoil to catch. The end result was that the parafoil deployed, but did not separate from the shock cord. There were simply too many lines in one place. So, this issue will be solved by moving the payload link away from the drogue link.

4.2 Payload Concept Features and Definition

4.2.1 Creativity and originality

While the use of energy scavenging schemes is in itself not novel, the windbelt ambient wind energy scavenging system that we propose is unique in several ways. Firstly, we will demonstrate the use and autonomous control of such a scheme on an airborne system. While it is relatively straightforward to install and maintain such energy scavenging devices on the ground, it is not immediately obvious whether such a system is practical to use on an aircraft. In addition, while the basic operating principle of a windbelt may, at first glance, appear simple, it is difficult to tell when such a system is optimized. In this experiment, we take a systematic approach to determining which factors affect the system's performance and the interrelationships between these factors.

While most modern windbelt energy scavenging systems are designed to generate electricity over a range of wind speeds, the performance is not optimized over this range. Our unique design will investigate the use of an active belt tuning system that aims to optimize the windbelt performance as the wind speed varies. This will be discussed in detail in later sections. In addition, bearings at the base of the UAV's wing assemblies (designed to support the windbelts, magnets, and coils) will be employed to passively orient the windbelts in the direction of maximum wind speed.

4.2.2 Significance

Since only one of two windbelts on the UAV will utilize the tuning scheme, the collected data (generated voltage, transmitted at regular intervals throughout UAV descent) will allow us to determine whether the performance of a windbelt system is significantly improved by using such active controls. It is important to determine whether the improvement in performance is considerable enough to justify the use of the active control system, which itself requires power to operate.

If this is found to be true, this may have significant applications to the improvement of ground-based windbelt energy scavenging systems used for power generation in developing countries, as well as those on airborne systems, which many be used to power various sensors and instrumentation on board the aircraft.

4.2.3 Suitable level of challenge

This experiment involves many challenging aspects. Primarily, many pre-flight tests must be conducted to investigate a variety of design options, ranging from the characteristics of the windbelt itself, to the magnet strength and placement. Various tradeoffs must be carefully considered, including those between such factors as the number of turns in the copper coils, magnet strength, belt tensile strength and weight of the wing assemblies and overall structure. Detailed testing must be carried out to accurately relate wind speed, belt tension, and belt oscillation modes. The accuracy of this empirical model will be crucial to the success of the active windbelt tuning system.

In addition, the mechanical challenges of designing, assembling and deploying the payload and wing structures, materials and weight considerations, the development of the software necessary to autonomously control the energy scavenging system throughout descent, and the transmission of voltage, GPS, and altitude data at regular intervals all pose a significant challenge to our team.

4.3 Science Value

4.3.1 Payload Objectives

The main objective of the payload is to analyze the effectiveness of an active control system for maximizing the power output of a windbelt energy scavenging system. Other objectives include investigating the relationship between various factors affecting the windbelt system's performance, and determining the practically of using such an energy scavenging scheme on an airborne system.

4.3.2 Success Criteria

Payload success criteria are as follows:

1) Payload is deployed successfully from rocket (complete separation, proper orientation)
2) Payload parafoil deployed successfully
3) Successful deployment and locking of windbelt wing assemblies following payload separation
4) Windbelt active control system autonomously adjusts tension in primary windbelt every three seconds beginning shortly after wing assemblies deploy and terminating prior to wing assembly retraction
5) Analog voltage from both primary and secondary windbelt systems is transmitted to ground station computer every five seconds beginning shortly after wing assemblies deploy and terminating prior to wind assembly retraction
6) Altitude and GPS data transmitted every five seconds from deployment to landing
7) Retraction of windbelt wing assemblies at a predetermined altitude prior to landing
8) Collected voltage data allows for a conclusion to be drawn regarding the effectiveness of the windbelt active control system

4.3.3 Experimental Logic, Approach, and Method of Investigation

Experimental Logic

In a basic windbelt system, a flexible belt is caused to oscillate by incident airflow. A permanent magnet attached to the belt moves relative to a conducting coil, thereby generating a voltage in the coil. We propose that the amount of power generated is strongly dependent on the mode of vibration of the belt. In particular, we believe that the generated power is maximized when the belt oscillates at its fundamental frequency. This will occur when the vortex shedding frequency of the airflow is matched to the fundamental frequency of the belt.

Approach

The goal of the experiment is to investigate whether the amount of power generated by a windbelt can be maximized by using an active control system to maintain the fundamental mode of vibration in the belt, even as the wind speed varies throughout descent. Tests will be conducted to directly relate an observed wind speed to the resonance frequency of a belt at a given tension. The details of this are discussed in the next section. Recalling that the fundamental frequency of a string is determined by its length, tension, and mass per unit length, we will also conduct tests to determine the analytical relation between these parameters for the belt used.

Based on this approach, the active control system will be designed to maintain the resonance condition between the vortex shedding frequency for a measured wind speed and the belt fundamental frequency by periodically adjusting the belt tension. The logic flow is shown graphically in Fig. 19.

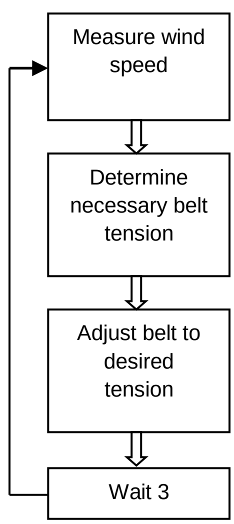

Figure 39 Logic flow of active belt tensioning system.

Investigation Method

In order to investigate our hypothesis, the UAV will have two separate wing assemblies, each with an independent windbelt system. The systems will be identical and symmetric. The “primary system” will utilize the active control mechanism to maintain a resonance with the incident airflow, while the “secondary system” will not. The voltage obtained from both windbelts will be transmitted to the ground station every 3 seconds throughout descent. The resulting data will be processed post-flight and analyzed for trends indicating higher power generation for the system which utilizes the active control mechanism versus that which does not.

4.3.4 Test and Measurement Methods, Variables, and Controls

Pre-Flight

Extensive testing will be carried out prior to launch. The goal of several of these tests will be to investigate design options. This will include testing various belt widths, magnet weight and strength, and magnet placement. In these tests, the belt tension and wind speed are kept constant and the oscillation modes and power generation are observed by measuring the resulting voltage waveform with an oscilloscope.

We will also carry out testing that will allow us to predict relationships between various variables of interest. These include the following:

1) Relationship between wind speed, belt tension, and belt fundamental frequency
2) Relationship between length, tension, mass per unit length, and oscillation frequency of belt

In the first case, we will vary the tension of a belt and apply a variable wind speed until the fundamental oscillation mode is observed for each tension. This will be determined both by visual observation and by monitoring the output voltage waveform. Wind speed will be controlled using a fan run by a variable speed motor.

In the second case, a belt of fixed length and mass will be adjusted over a range of tensions and excited by plucking. The resulting frequency of oscillation will be measured by looking at the frequency of the resulting voltage waveform. The data will be compared to the analytical model of oscillation modes on an elastic string.

In-Flight

Throughout the payload descent, voltage generated by each of the symmetric windbelt systems will be converted to DC using a full wave rectifier circuit, and then measured using an Arduino Nano microcontroller. The measured values will be transmitted to the ground station computer every five seconds. Post flight, the power output data for the actively controlled windbelt system will be compared to that of the secondary system. This secondary system represents the control variable of the experiment. The average power output of the secondary system will give us a baseline value for the generated power. This value will allows us to determine whether or not the use of the active control system improved the windbelt system's performance.

4.3.5 Relevance of Expected Data

The expected data will allow us to determine whether the performance of a windbelt system depends on the oscillation mode of the belt, and whether such a system's performance may be optimized by utilizing an active control scheme to tune the belt to the resonant frequency of the incoming airflow. Clearly, an active control system requires power to operate, and the question to be answered is whether the gain in generated power is significant enough to justify the use of such a system. While our system is mainly a proof-of-concept, a larger system that generates relatively large amounts of power may be able to produce several times the amount of energy by employing a tuning scheme. In such a case, the power necessary to run the control system would be far outweighed by the gain in energy output.

4.3.6 Accuracy and Error Analysis

The expected voltage data will have relatively small values (on the order of mV), so that we anticipate a moderate amount of noise to be present in each measurement. However, since we are only interested in overall trends and the relationship between the data for the primary and secondary windbelts, this should not be a problem. Each dataset will be averaged post flight, and these average values will be compared to determine whether there was a significant difference in power generation between the two systems.

4.3.7 Preliminary Experimental Process Procedure

The experimental process procedure for the in-flight energy scavenging system test will be as follows:

1) Visually confirm deployment and locking of windbelt wing assemblies
2) Confirm start of voltage data transmission (will commence autonomously once wings have deployed and locked)
3) Monitor and record voltage data throughout descent
4) Confirm termination of voltage data transmission (will occur autonomously based on altitude data)
5) Visually confirm retraction of wing assemblies

4.4 Safety and Environment (Payload)

The primary concern with the payload is successful deployment of the recovery system. Otherwise, the payload poses no environmental hazard if successfully recovered. Please refer to the Safety and Evironment (Vehicle) section for further information.

5.0 Launch Operations Procedures

5.1 Checklist

The vehicle will be mounted with rail buttons on a 15-Series 80/20 based launch rail. The total length of the rail is 12-Feet and is figured in to all simulations. The vehicle's motor will be ignited remotely by the range firing system provided.

Proper Assembly Procedures

The planned steps for assembly of the vehicle are as follows:

1. Prepare Avionics and Sustainer
    a. Prepare Main ejection charges on top Avionics Bulkhead
    b. Connect main ejection charges to flight computers
    c. Connect main parachute shock cord with quick link to top Avionics Bulkhead U-bolt
    d. Insert electronics sled in to Sustainer with top Avionics Bulkhead
    e. Prepare Apogee ejection charges
    f. Connect Apogee ejection charges to flight computers

g. Insert Bottom Avionics Bulkhead in to Sustainer
h. Secure with washers and nuts
i. Connect electronics to switches mounted in hatch
j. Replace hatch with screws

2. Prepare Nosecone
    a. Attach main parachute shock cord to U-bolt of Nosecone
    b. Attach Main parachute with quick link to Nosecone
    c. Secure tracking electronics in Nosecone (BRB 900)
    d. Secure Nosecone Bulkhead with Screws
3. Pack Main Parachute and shock cord in to forward section of sustainer
4. Fit Nosecone to sustainer with shear pins
5. Prepare Booster Section
    a. Attach Drogue shock cord to forged Eye-bolt of engine block.
    b. Attach Drogue parachute to shock cord
    c. Attach Payload release mechanism to shock cord
    d. Fit payload in to booster with shock cord bypassing through channel
6. Fit Sustainer with Nosecone over booster and secure with shear pins

Flight Computers

Verify flight computer configurations	___
Replace Flight Computer Batteries	___
Check Battery Voltage	___
Check Flight Computers	___
Wire E-Matches	___
Set Charges	___

GPS

Activate/check battery voltage	___
Connect Antenna to receiver	___
Mount Antenna	___
Connect Receiver to laptop Serial connection	___
Confirm GCS Link	___
Place transmitter in casing	___
Insert in Nosecone communication bay	___

Avionics Bay

Replace Electronics bay in airframe	___
Rewire Flight computers to key switches	___

Recovery System

Insert Nomex wadding	___

Prepare main parachute ___
--Fold ___
--Place in bag ___
--Gather Shroud Lines ___
--Connect to top of AV-Bay ___
--Place in forward bay ___

Connect Main chute to nosecone ___
Place drogue in rear sustainer bay ___
Gather shock cord in airframe ___
Position nosecone ___
--Insert shear pins ___

Payload

Activate Experimental Payload ___
Insert Experimental Payload in rear bay ___
Position Sustainer on Booster ___
--Insert shear pins ___

Loading Motor

Place Motor in motor mount tube ___
Lock engine retainer ring ___
Insert igniter rod through center of engine grains to top ___
Tape igniter rod into place ___
Visually confirm ignition system disconnected (saftied) ___
Unshort leads ___
Connect to ignition system ___

Launch Procedure

Load vehicle on launch Rail ___
Angle launch rail to vertical ___
Activate Flight Computers ___
Clear launch pad ___
Confirm continuity ___
Signal launch readiness ___

Post Flight Recovery and Inspection

Visually mark touchdown location ___
Distribute Walkie Talkies ___
Deploy Recovery Team ___
Guide Recovery Team to Rocket ___
Confirm recovery of rocket to GCS ___

Saturate Unexploded BP with water ___
Deactivate secondary Flight Computer ___
Record altitude given by primary Comptuter ___
Deactivate Primary altimeter ___
Return Vehicle to GCS for inspection ___
Inspect vehicle for critical damage ___
Deploy recovery team to Payload ___
Guide recovery team to payload ___
Confirm recovery of payload to GCS ___
Return Payload to GCS for inspection ___

6.0 Activity Plan

6.1 Budget Plan

Currently, the total estimated expense of the project is $10,000. This is divided between project supplies, fabrication, testing and projected travel expenses. The project supplies, fabrication and testing have been allocated on a team basis. This amounts to $7,000 of the total budget and the list of anticipated supplies is listed in Table 7 on the following page.

The primary source of the project funding is be derived from the $10,000 NASA Nebraska Minigrant. Additionally, $500 of this has been raised from other sources. So far, $400 has been donated to the chapter by corporate sponsors and $120 from volunteering at the Guardian's of Freedom Air Show. This funding primarily goes towards the overhead of running the club. The team has successfully covered any previous gap in funding.

Travel and accommodations for 6 team members to the competition is estimated at $2,000. This will include van rental, gas, three hotel rooms, and meals. Hotel rooms have already been covered. And the team is renting a van to travel down to Huntsville. The money reserved for this currently $1100. This will be used to cover the rental, gas, and some meals.

Table 2 Projected project expenses and current expenditures.

Sub-group	Item Needed	Price	#	Estimate	# Purchased	Purchase Cost
Airframe	BT 5.5in	56.95	2	113.9	2	113.9
(allocated:$2000)	BT Coupler	55.95	1	55.95	1	55.95
(Updated 1/25/2012)	Kevlar Sock(per ft)	3.51	24	84.24	30	105.22
	Glass Sock(per ft)	1.8	16	28.8	25	45.04
	98 mm MMT	15.47	1	15.47	2	30.95
	75 mm MMT	14.49	0	0	1	14.49
	5 mm Plywood 4x8	10	1	10	1	11.63
	All-Thread	6	3	18	1	5.99
	U-Bolts	5	4	20	3	3.9
	Misc Hardware	50	1	50		18.41
	Main Parachute	150	1	150		
	Shock Cord	3	50	150	30	21
	Drogue Chute	40	1	40	1	43
	Nosecone Mold	30	1	30	1	120
	Subtotal Estimate			766.36	Current Subto	589.48
Avionics	Flight Computer A	100	1	100	1	66
(allocated:$1250)	Flight Computer B	155	1	155	1	75.5
(Updated 1/25/2012)	Key Switches		2	0	3	15
	Batteries	11	4	44	4	44
	Antenna	20	1	20		
	Transciever	70	2	140		
	Electronic Compone	25	1	25		16
	GPS	30	1	30		400
	Subtotal Estimate			514	Current Subto	616.5
Payload	Ram-Airfoil	75		0		
(allocated:$2000)	Servos	30	6	180		
	Arduino	40	2	80		80
	Sensors	400	1	400		
	Antenna	20	2	40		
	Transciever	70	2	140		
	Misc Components	610	1	610		
	Subtotal Estimate			1450	Current Subto	0
Propulsion	L-Class Motor	200	2	400		
(allocated:$1000)	75 mm Motor Hardv	300	1	300		
(Updated 1/25/2012)						
	Subtotal Estimate			840	Current Subto	0
Outreach	Water Rocket Pad	120	1	120	1	100
(allocated:$250)	Stomp Rockets	50	1	50		
(Updated 1/25/2012)	Misc Supplies	80	1	80		
	Subtotal Estimate			250	Current Subto	100
			Total	3820.36	Current Total	$ 1,305.98
					Allocated Tota	$ 7,000.00

6.2 Timeline

Planning for the UNL Rocketry Team's entry into the USLI competition began immediately after completion of the IREC competition in June. Since that time, the project director has secured funding and the team has designed a vehicle that fulfills the mission requirements. The team became organized and filled out since the beginning of the fall semester. Since then the whole UNL Rocketry Team has met on a weekly basis. The sub-teams have been divided in responsibility to reduce interdependence but bolster cooperation through shared membership. This was made possible through extensive planning. These teams have also begun meeting independently to solve their assigned tasks.

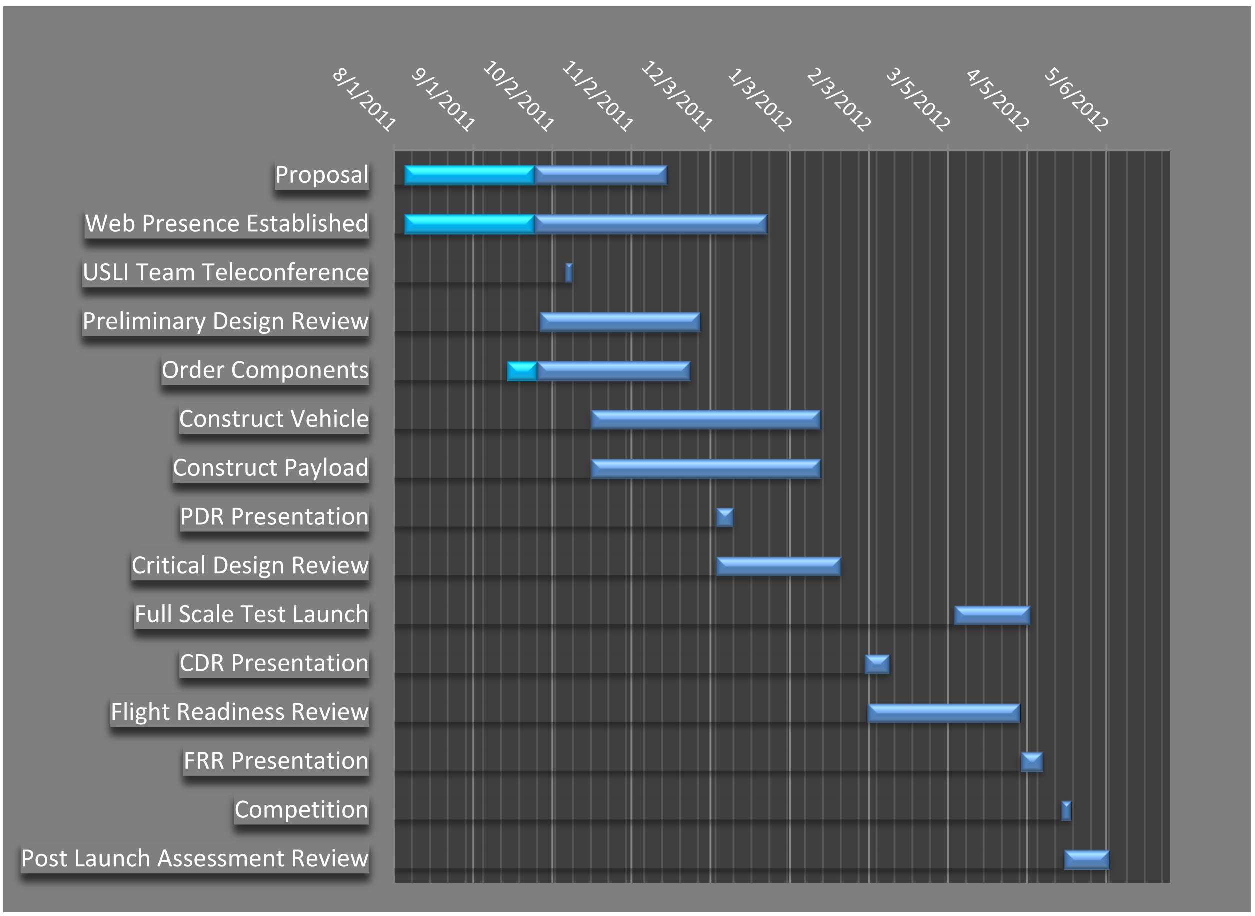

Figure 40 Gantt chart of project tasks.

6.3 Educational Engagement #1

The first day working with students was basic. We discussed how the water rockets worked so they could fully understand the safety precautions that were needed to be taken. After covering safety we built a rocket in a step by step process in front of the class. By doing this we could show the entire class the tricks of construction that we have learned over the years.

The next day the class finished the construction of the rockets. We then did some preliminary air tests by tilting the launch pad sideways and launching rockets horizontally down the hallway. We also showed the students that making hemispherical fins can make the rocket rotate analogous to rifling bullets.

Figure 41 Launching rockets down hallway.

Figure 42 Picture of some involved students with completed rockets.

The final day we inspected the rockets and made sure they were ready to fly. We then went out to the middle schools soccer field and launched the rockets. Most of them were unbalanced and in result didn't fly very successful. However we had a few that flew beautifully and we used the differences in the unsuccessful and successful rockets to teach the kids how to improve the rocket.

In the end we told the students, "This process of repetitive adjustments and improvements to the rocket is engineering". That makes everyone in this class an engineer!

6.4 Educational Engagement #2

Introduction

Teaching today has turned from pursuing your interests to memorizing the required. As I sit in class everyday I think about where I would be if I didn't have someone or something to inspire me to learn. That is why I headed up the outreach projects for this years team. Unlike in the fall where we spent 3 days on teaching, designing and building, we shove it all into one day. We spent that one-day (3/20/12) on inspiring and telling the students about our experiences with the rocket and got the students fired up about building stomp rockets.

Capturing the students interest

Paul and I started the class by getting the students attention and walked in with the subscale USLI Rocket. The “ooohs” and “awwwhs” filled the room and we got students attention immediately. Paul and I discussed the entire rocket from the nosecone to the fins and retainer. As we got deeper on how the rocket worked, students started asking questions and that is when we knew that we got a hold of their interest. When we were done speaking about the subscale USLI Rocket, we watched videos of “balls” and “LDRS” high-powered rocketry launches. We explained what the amateurs did to prepare the rocket, why they launched and what made the rocket successful with a recover system.

After the video, we brought in “Deimos” our main USLI rocket into class. We invited the students up to the front of the class and they were very excited. We compared and contrasted the subscale, full-scale and “LDRS” rockets. We answered questions about the structural integrity, recovery systems, computer systems, and how the motor works.

Activity

The overall presentation went very well. We captured the student’s young minds and we embellished their curiosity by asking them to engineer a paper stomp rocket. You are probably wondering, what is a stomp rocket? Well you first build a launch paunch/ fuel containment device or 2L bottle containing air and a foot for the external force. You take two .848”outside diameter corner PVC pipes connected with one .625” outer diameter 5” long PVC pipe. Then attach one more straight .625” outer diameter PVC and use that for the nipple. Your U shape PVC pipe will have one end, without the nipple, be placed into the tip of the 2L bottle. The other end will be the nipple facing the direction of trajectory. The rockets themselves are made from scratch paper, wrapped around the nipple PVC pipe and then taped. Cut out some fins and a nose cone and you have a rocket.

Conclusion

We decided to compete to see whose rocket would go the farthest. Unfortunately the class ended and we were unable to see the students compete. All in all it was a very touching experience to not just entertain students with rockets, I got to inspire students to learn and be curious. With this being our second educational engagement we tallied up a total of 121 students affected by the University of Nebraska-Lincoln USLI team.

7.0 Conclusion

Figure 43 All associated equipment and hardware for the project.

Overall, the project is moving forward as expected and has become more promising. The additional funding has afforded greater freedom in the design and more testing to take place. The vehicle has been built, ground tested, and flight tested successfully. The payload system will also prove to be quite insightful in to aircraft mounted tuned windbelts used for energy scavenging.

The conclusion drawn from the test flight is that the vehicle is ready to be flown at the competition. The test flight has revealed that the surface drag of the vehicle is higher than originally modeled and reduces the altitude obtained substantially. The refined simulation shows the L-1170 motor still has enough total impulse for the mission at hand but the team is prepared to employ a motor with greater energy is needed. This will allow a larger payload and accommodate any unforeseen growth in mass we may encounter. It can also be seen that the vehicle maintains a fair margin of stability all the way through the ascent of the flight. The recovery systems for the vehicle operated as intended and the payload recovery only needs to be moved in the vehicle in order to separate properly. With the lessons learned from this, the team is certainly able to fly the vehicle safely and reliably.

Figure 44 Recovery hardware of rocket deployed and the payload parafoil being released.

Appendix – OpenRocket Part Detail

Parts Detail

Sustainer

Nose cone	Fiberglass (1.85 g/cm^3)	Haack series	Len: 27.5in	Mass: 1.719lb
Bulkhead	Plywood (birch) (0.63 g/cm^3)	Dia_{out} 5.343in	Len: 0.25in	Mass: 0.128lb
Nose Tube	Kraft phenolic (0.95 g/cm^3)	Dia_{in} 3.961in Dia_{out} 4in	Len: 18in	Mass: 0.152lb
Bulkhead	Plywood (birch) (0.63 g/cm^3)	Dia_{out} 3.961in	Len: 0.25in	Mass: 0.07lb
Comm Systems		Dia_{out} 1.181in		Mass: 2.5lb
Centering ring	Plywood (birch) (0.63 g/cm^3)	Dia_{in} 4in Dia_{out} 5.343in	Len: 0.25in	Mass: 0.056lb
Centering ring	Plywood (birch) (0.63 g/cm^3)	Dia_{in} 4in Dia_{out} 5.343in	Len: 0.25in	Mass: 0.056lb
Tube coupler	Kraft phenolic (0.95 g/cm^3)	Dia_{in} 5.232in Dia_{out} 5.31in	Len: 8in	Mass: 0.179lb
Body tube	Quantum tubing (1.05 g/cm^3)	Dia_{in} 5.3in Dia_{out} 5.5in	Len: 48in	Mass: 3.089lb
Booster Coupler	Fiberglass (1.85 g/cm^3)	Dia_{in} 5.2in Dia_{out} 5.3in	Len: 12in	Mass: 0.661lb
Payload 10 lb		Dia_{out} 5.2in		Mass: 9.5lb
Parachute	Ripstop nylon (67 g/m^2)	Dia_{out} 108in	Len: 9.449in	Mass: 2.76lb
Shroud Lines	Tubular nylon (11 mm, 7/16 in) (13 g/m)	Lines: 16	Len: 162in	
Shock cord	Tubular nylon (25 mm, 1 in) (29 g/m)		Len: 624in	Mass: 1.013lb
Shock cord	Tubular nylon (25 mm, 1 in) (29 g/m)		Len: 360in	Mass: 0.585lb
Drogue Parachute	Ripstop nylon (67 g/m^2)	Dia_{out} 36in	Len: 3.11in	Mass: 0.237lb
Shroud Lines	Tubular nylon (11 mm, 7/16 in) (13 g/m)	Lines: 4	Len: 48in	
Avionics Bay	Kraft phenolic (0.95 g/cm^3)	Dia_{in} 5.182in Dia_{out} 5.3in	Len: 12in	Mass: 0.4lb
Bulkhead	Plywood (birch) (0.63 g/cm^3)	Dia_{out} 5.182in	Len: 0.25in	Mass: 0.12lb
Bulkhead	Plywood (birch) (0.63 g/cm^3)	Dia_{out} 5.182in	Len: 0.25in	Mass: 0.12lb
Bulkhead	Plywood (birch) (0.63 g/cm^3)	Dia_{out} 5.382in	Len: 0.25in	Mass: 0.129lb
Bulkhead	Plywood (birch) (0.63 g/cm^3)	Dia_{out} 5.382in	Len: 0.25in	Mass: 0.129lb

Inner Tube	Kraft phenolic $(0.95\ g/cm^3)$	Dia_{in} 3.858in Dia_{out} 4in	Len: 11.5in	Mass: 0.345lb
Avionics Mass		Dia_{out} 1.181in		Mass: 1.5lb
Booster Section	Fiberglass $(1.85\ g/cm^3)$	Dia_{in} 5.3in Dia_{out} 5.5in	Len: 48in	Mass: 5.442lb
Freeform fin set (3)	Plywood (birch) $(0.63\ g/cm^3)$	Thick: 0.197in		Mass: 0.652lb
Inner Motor Mount Tube	Kraft phenolic $(0.95\ g/cm^3)$	Dia_{in} 3.858in Dia_{out} 4in	Len: 36in	Mass: 1.081lb
Engine block	Plywood (birch) $(0.63\ g/cm^3)$	Dia_{in} 5.3in Dia_{out} 5.3in	Len: 0.5in	Mass: 0lb
Centering ring	Plywood (birch) $(0.63\ g/cm^3)$	Dia_{in} 4in Dia_{out} 5.3in	Len: 0.5in	Mass: 0.108lb
Centering ring	Plywood (birch) $(0.63\ g/cm^3)$	Dia_{in} 4in Dia_{out} 5.3in	Len: 0.5in	Mass: 0.108lb
Centering ring	Plywood (birch) $(0.63\ g/cm^3)$	Dia_{in} 4in Dia_{out} 5.3in	Len: 0.5in	Mass: 0.108lb
Centering ring	Plywood (birch) $(0.63\ g/cm^3)$	Dia_{in} 4in Dia_{out} 5.3in	Len: 0.5in	Mass: 0.108lb
Centering ring	Plywood (birch) $(0.63\ g/cm^3)$	Dia_{in} 4in Dia_{out} 5.3in	Len: 0.5in	Mass: 0.108lb
Launch lug	Polycarbonate (Lexan) $(1.2\ g/cm^3)$	Dia_{in} 0in Dia_{out} 0.394in	Len: 1.181in	Mass: 0.006lb
Launch lug	Polycarbonate (Lexan) $(1.2\ g/cm^3)$	Dia_{in} 0in Dia_{out} 0.394in	Len: 1.181in	Mass: 0.006lb